

MULTI-OBJECTIVE LARGE LANGUAGE MODEL ALIGNMENT WITH HIERARCHICAL EXPERTS

000
001
002
003
004
005 **Anonymous authors**
006 Paper under double-blind review
007
008
009
010

ABSTRACT

011 Aligning large language models (LLMs) to simultaneously satisfy multiple ob-
012 jectives remains a significant challenge, especially given the diverse and often
013 conflicting nature of human preferences. Existing alignment methods struggle to
014 balance trade-offs effectively, often requiring costly retraining or yielding subopti-
015 mal results across the Pareto frontier of preferences. In this paper, we introduce
016 HoE (Hierarchical Mixture-of-Experts), a *lightweight, parameter-efficient*, and
017 *plug-and-play* approach that eliminates the need for model training, while enabling
018 LLMs to adapt across the entire Pareto frontier and accommodate diverse user
019 preferences. In particular, HoE consists of three hierarchical components: LoRA
020 Experts, Router Experts and Preference Routing, reaching state-of-the-art Pareto
021 frontiers and achieving a trade-off between parameter size, training cost, and per-
022 formance. We evaluate HoE across various tasks on 16 objectives and 200 different
023 preferences among 8 benchmarks, demonstrating superior performance over 15
024 recent baselines. **WARNING: This paper contains potentially offensive text.**
025
026

1 INTRODUCTION

027 Large language models (LLMs) have achieved remarkable success in aligning with broadly defined
028 human values (Achiam et al., 2023; Ziegler et al., 2019; Sun et al., 2023). However, human preferences
029 in practice are highly diverse and cannot be fully captured by an universal alignment goal. Users may
030 pursue multiple personalized objectives, and even when the objectives are the same, their relative
031 importance often varies across individuals and contexts (Fu et al., 2024; Yang et al., 2024c; Lin et al.,
032 2025; Ren et al., 2025; Zhang et al., 2025). Existing approaches (Sun et al., 2023; Yang et al., 2025;
033 Chen et al., 2025), which typically optimize for one objective or a fixed combination, fall short in
034 flexibly covering this preference space. These observations highlight the necessity of multi-objective
035 alignment (MOA) to enable scalable and preference-steerable LLMs (Lin et al., 2025; Guo et al.,
036 2024; Ramé et al., 2023; Jang et al., 2023; Yang et al., 2024c; Lin et al., 2025; Chen et al., 2025).

037 The central difficulty of multi-objective
038 alignment (MOA) lies in its inherently
039 steerable nature: LLMs must dynamically
040 adapt to arbitrary user preferences rather
041 than a single fixed goal, essentially acting
042 as a “jack-of-all-trades” (Lin et al.,
043 2025; Chen et al., 2025). This steerability
044 introduces two major challenges. *First, objectives often conflict with each other.*
045 Parameters tuned to improve one objective
046 (e.g., helpfulness) often undermine another
047 (e.g., harmlessness) (Chen & Kwok,
048 2025; Zheng & Wang, 2024; Guodong
049 et al., 2024; Yadav et al., 2023; Zhou et al.,
050 2024a). *Second, competition also even exists across preferences along the Pareto frontier* (Wang et al., 2024b; Shi et al., 2024; Zhou et al., 2024b; Li et al., 2021).
051 For instance, a model trained uniformly

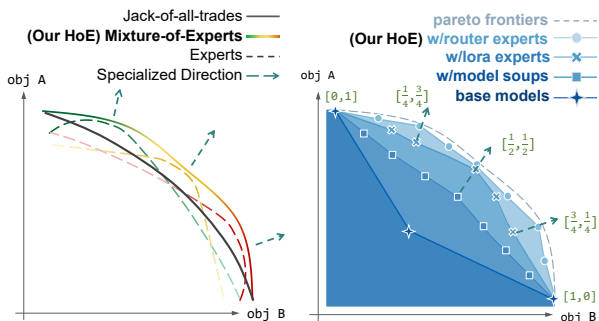


Figure 1: (Left) HoE decomposes the multi-objective alignment problem into a series of single-preference subproblems, each handled by a specialized expert. (Right) HoE employs hierarchical experts, integrating LoRA and router experts to approach near-optimal Pareto frontier.

054 across all weightings (black solid Pareto Frontier in Fig. 1 Left) cannot achieve optimal performance
 055 at a specific weighting (e.g., [0.5, 0.5]), compared to the expert model fine-tuned exclusively for that
 056 preference (colored dashed Pareto frontier in Fig. 1 Left).

057 To overcome this limitation, we adopt a decomposition-based strategy for MOA, breaking down
 058 the multi-objective alignment problem into a series of single-preference subproblems (Zhang &
 059 Li, 2007), each associated with a set of specialized parameters. These parameters, referred to as
 060 experts, are each assigned to a distinct preference, focus solely on their corresponding preferences
 061 and optimize within their localized subproblem regions. This strategy avoids the pitfalls of a single
 062 monolithic model attempting to cover the entire Pareto Frontier, thereby circumventing the steerability
 063 bottleneck.

064 Building on this idea, we then instantiates each expert as a lightweight LoRA adapter within a
 065 Mixture-of-Experts framework. Preference-specific behavior is captured in small, composable LoRA
 066 modules while the backbone parameters remain shared. At inference time, a preference-conditioned
 067 routing mechanism composes and activates the appropriate LoRA experts, adapting the model’s
 068 behavior dynamically to realize arbitrary weightings. By this design, we efficiently reconstruct the
 069 full Pareto frontier from a collection of localized, preference-specific experts, enabling a scalable,
 070 steerable, and parameter-efficient approach for multi-objective alignment.

071 In this work, we propose $\text{H}\circ\text{E}$, a novel hierarchical Mixture-of-Experts framework for multi-objective
 072 alignment. $\text{H}\circ\text{E}$ is a *lightweight, parameter-efficient, and plug-and-play* solution that eliminates the
 073 need for training any models while achieves strong performance across the entire Pareto frontier. It
 074 combines the decomposition principle with the LoRA-based MoE design to enable scalable, efficient
 075 and fine-grained control over the entire Pareto frontier. Specifically, $\text{H}\circ\text{E}$ comprises three hierarchical
 076 components: LoRA experts, router experts, and preference routing. (1) “LoRA experts” are first
 077 extracted *without training* from off-the-shelf single-objective models using task-vector singular value
 078 decomposition (task-SVD), capturing distinct alignment objectives in compact adapter modules. (2)
 079 “multi-objective LoRA experts” are then synthesized, also *without training* by merging multiple
 080 existing single-objective LoRA experts, to enable on-demand generation of alignment capabilities
 081 across arbitrary preference configurations. (3) “Router experts” are trained with negligible parameters
 082 to dynamically select and combine the appropriate experts based on user-specified preferences,
 083 allowing efficient traversal of the Pareto frontier. Through this hierarchical design, $\text{H}\circ\text{E}$ not only
 084 provides precise control over preference-specific behavior but also balances alignment performance,
 085 parameter cost, and training efficiency. It serves as a practical and effective solution for scalable
 086 multi-objective alignment in LLMs.

087 The main contributions of this study are as follows:

- 088 • We investigate a novel decomposition strategy that breaks down the multi-objective alignment
 089 problem into a series of single-preference subproblems, each handled by a set of specialized
 090 experts, enabling fine-grained control and full Pareto coverage.
- 091 • We propose $\text{H}\circ\text{E}$, a *lightweight, parameter-efficient* and *plug-and-play* hierarchical Mixture-of-
 092 Experts framework that comprises three-level hierarchy, bypassing full model training.
- 093 • We evaluate $\text{H}\circ\text{E}$ across diverse multi-, many-objective and multi-task settings, involving 14
 094 objectives, 6 benchmarks, and 200 preference. $\text{H}\circ\text{E}$ consistently outperforms 15 recent
 095 baselines with lower training cost and parameter overhead.

097 2 RELATED WORK

098 **LLM Multi-objective Alignment.** MORLFH (Li et al., 2021) and MODPO (Zhou et al., 2024b)
 099 employ linear scalarization to combine multiple reward signals into a single scalar metric, applying
 100 standard RLHF or DPO training a separate model for each preference. Multi-objective Decoding
 101 (MOD) (Shi et al., 2024), Alignment as Reward-Guided Search (Args) (Khanov et al., 2024) and
 102 Personalized Alignment at Decoding-time (PAD) (Chen et al., 2025) derive a closed form solution of
 103 optimal preference model and perform linear fusion of logits prediction during decoding. Directional
 104 Preference Alignment (DPA) (Wang et al., 2024a) and Reward-in-Context (RiC) (Yang et al., 2024c)
 105 typically inject user preferences into the prompt, enabling in-context preference-conditioned align-
 106 ment. Additionally, Steering (Konen et al., 2024; Rimsky et al., 2024) adding “steering vectors” to
 107 all token positions after the user’s prompt, enabling precise control over multi-objective preferences.

108 Table 1: Comparison with other alignment methods. M is number of preference, N is number of
 109 objectives and $M \gg N$. Our $\text{H}\circ\text{E}$ approach is a pareto-steerable and lightweight method with highest
 110 scalability, least storage cost and least inference cost, which eliminates the need for retraining any
 111 new models or any structured prompts. Each characteristic is empirically conformed in Section B.5.

Characteristic (\rightarrow) Method (\downarrow)	Number of stored models	Inference cost	Number of trained models	Pareto steerable	Multi-task ability	Scalability	Free from prompting
MORLHF [IEEE 21]	M	1	M	✓	✗	Retrain	✓
MODPO [ACL 24]	M	1	M	✓	✗	Retrain	✓
RS [NeurIPS 23]	N	1	0	✓	✓	✓	✓
RiC [ICML 24]	>1	1	>1	✓	✗	Retrain	✗
DPA [ACL 24]	1	1	1	✓	✗	Retrain	✗
MOD [NeurIPS 24]	N	N	0	✓	✓	✓	✓
Args [ICLR 24]	0	>N	0	✓	✗	✓	✓
Steering [EACL 24]	0	1	0	✗	✗	✓	✓
MetaAligner [NeurIPS 24]	1	2	1	✗	✗	✓	✗
LoraMoE [ACL 24]	1	1	1	✗	✓	Retrain	✓
PCB-Merging [NeurIPS 24]	1	1	0	✗	✓	✓	✓
PAD [ICLR 25]	1	3	1	✗	✗	Extra-train	✗
GenARM [ICLR 25]	0	>N	0	✓	✗	✓	✓
PARM [ICML 25]	0	2	1	✓	✗	Retrain	✓
H$\circ\text{E}$ (ours)	1	1	0	✓	✓	✓	✓

127
 128 MetaAligner (Yang et al., 2024b) extends the Aligner (Ji et al., 2024) framework to MOA, refining
 129 weaker outputs to better match user preferences.

130
 131 **Knowledge Fusion for LLMs.** Model merging (Jin et al., 2022; Matena & Raffel, 2022; Guodong
 132 et al., 2024; Zheng & Wang, 2024; Yadav et al., 2023) is a widely used fusion technique that integrates
 133 multiple task-specific models into a unified model. Task Arithmetic (TA) (Ilharco et al., 2023; Ramé
 134 et al., 2023; Jang et al., 2023) linearly combines task vectors, defined as the parameter differences
 135 between task-specific models and the original pre-trained model. Then Rewarded Soups (RS) (Ramé
 136 et al., 2023) and Personalized Soups (PS) (Jang et al., 2023) firstly extend this concept to MOA.
 137 LoraMoE (Dou et al., 2024), the closest work to ours, is a Mixture-of-Experts (MoE) approach
 138 that uses LoRA Adapters (Hu et al., 2022) as experts, integrating LLM knowledge by activating
 139 select experts via a router network. However, it requires costly training across all LoRA experts
 140 simultaneously and limits knowledge sharing among them, thus unsuitable for MOA.

141 In summary, we systematically compare and analyze existing LLM alignment methods in Tab. 1.

142 3 METHODOLOGY

144 In this section, we present the methodology behind $\text{H}\circ\text{E}$, a lightweight, parameter-efficient, and
 145 plug-and-play multi-objective alignment framework. As illustrated in Fig. 2, our $\text{H}\circ\text{E}$ approach
 146 consists of three *hierarchical* components: LoRA experts, router experts and a preference routing.

148 **Multi-Objective Alignment Problem Setting.** In the MOA setting, we consider N alignment
 149 objectives with reward functions $\{R_i(\cdot)\}_{i=1}^N$. A user preference is represented by a weight vector
 150 $\lambda^{\text{usr}} = (\lambda_1, \dots, \lambda_N) \in \Delta^{N-1}$ in the N -dimensional simplex, and is specified as a preference
 151 weighted reward: $R_\lambda(x, y) = \sum_{i=1}^N \lambda_i R_i(x, y)$. The objective of MOA is to learn a policy that
 152 aligns with arbitrary preferences λ across the simplex: $\max \mathbb{R}(\theta; \lambda) = \mathbb{E}_{y \sim \pi(\cdot|x; \lambda)} [R_\lambda(x, y)]$.

154 3.1 Primary LORA EXPERTS

155 **Single-Objective LoRA Experts. 1) Extraction.** We begin with a pre-trained model π_{pre} , and
 156 a collection of off-the-shell single-objective optimal policies $\{\pi_1^*, \dots, \pi_N^*\}$, each fine-tuned on its
 157 respective objective.

$$\pi_i^* = \arg \max_{\pi_\theta} \mathbb{E}_{x \sim D} [\mathbb{R}_i(\theta) - \beta \mathbb{KL}(\pi_\theta || \pi_{\text{pre}})] \quad (1)$$

161 Let θ_{pre} denote the pretrained parameters and let θ_i be the parameters of the fine-tuned model.
 Following the task vector paradigm in model merging (Ilharco et al., 2023), we define each *objective*

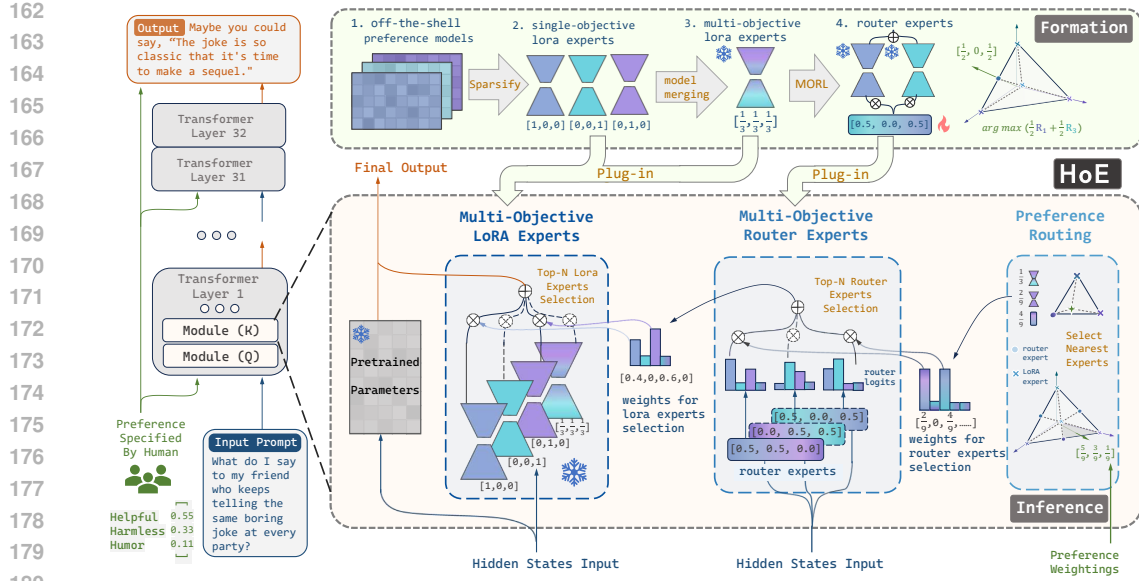


Figure 2: Illustration of our HoE approach. The left side illustrates the application scenario, where the model generates a response aligned with the prompt and given preferences. The bottom-right highlights its three **hierarchical** components - the LoRA experts, router experts, and a preference routing. The top-right depicts individual components, each serving as an expert for specific weightings, designed for seamless plug-and-play integration within the model.

vector as the parameter update between fine-tuned weights and the pre-trained weights:

$$\tau_i = \theta_i - \theta_{\text{pre}}, \quad (2)$$

which inherently capture the single-objective capabilities of each single-objective model.

2) Compression. Each objective vector τ_i is then compressed into a low-rank adapter via a task-aware truncated SVD procedure (“task-SVD”): $A_i, B_i \leftarrow \text{task-SVD}(\tau_i)$, where $A_i \in \mathbb{R}^{d_{\text{in}} \times r}$, $B_i \in \mathbb{R}^{r \times d_{\text{out}}}$ and $r \ll \min(d_{\text{in}}, d_{\text{out}})$. In practice, task-SVD selects high-magnitude components of τ_i , performs per-layer SVD truncation and rescales the parameters to form new LoRA matrices A_i, B_i . This compression preserves the optimal single-objective performance with negligible performance loss (cf. Wang et al. (2024c); Ping et al. (2024); Gu et al. (2025); Yuan et al. (2023); Ryu et al. (2023)). These compact adapters, referred to as LoRA Experts, are highly specialized for their corresponding objectives.

3) Plugin. We convert all linear layers in the Transformer into MoE-style plugin modules, incorporating the LoRA experts. Given a score weight $w^{(1)} \in \mathbb{R}^N$ from the router, the module output for input $x \in \mathbb{R}^{d_{\text{in}}}$ composes the pretrained weight with a weighted sum of LoRA experts:

$$O_{\lambda}(x) = W_{\text{pre}} x + \sum_{i=1}^N \lambda_i B_i(A_i x), \quad (3)$$

where $W_{\text{pre}} \in \mathbb{R}^{d_{\text{in}} \times d_{\text{out}}}$ is the base linear weight and $B_i A_i x$ is the low-rank residual from expert i .

Multi-Objective LoRA Experts. For preferences involving multiple objectives simultaneously, the aforementioned linear combination of single-objective experts may fail to recover optimal performance, especially at intermediate points on the Pareto frontier (e.g., $\lambda = [0.5, 0.5]$). To address this, we draw inspiration from model merging (Yang et al., 2024a; Matena & Raffel, 2022; Zheng & Wang, 2024; Guodong et al., 2024; Jin et al., 2022; Yadav et al., 2023) which amplify parameters beneficial to all tasks while suppressing conflicting or detrimental ones, enable nonlinear and fine-grained parameter adaptation, and significantly outperform linear approaches (e.g., Task Arithmetic (Ilharco et al., 2023)).

To cover the entire Pareto frontier, we incorporate model merging into our framework to derive new expert parameters tailored to arbitrary preference vectors. Given a target preference λ , we specify the

216 desired objective proportions and synthesize a merged expert with parameters:
 217

$$218 \quad \tau_\lambda = \text{Merge}(\{\tau_i\}_{i \in [N]}, \lambda) \quad (4)$$

219 where $\{\tau_i\}$ are the objective vectors derived from single-objective model. We then reuse the same
 220 task-SVD procedure. These resulting adapters serve as multi-objective LoRA experts, and are no
 221 longer aligned with a single objective, but instead specialized in specific combinations of objectives
 222 (e.g., $[0.5, 0.5]$).
 223

224 **3.2 Secondary ROUTER EXPERTS**
 225

226 While increasing the number of LoRA experts can improve Pareto coverage, the overall parameter
 227 budget quickly becomes prohibitive, as each adapter still adds a non-trivial number of parameters. To
 228 address this, we introduce *Router Experts*, a lightweight and fine-grained decomposition mechanism
 229 as secondary experts. Their parameter cost is negligible compared to LoRA adapters, yet they play
 230 a crucial role in enhancing flexibility: unlike LoRA experts, which are statically combined and
 231 tied to fixed preferences, router experts enable *module-wise fine-grained routing* and *input-adaptive*
 232 *selection*. In practice, this allows the model to dynamically determine which LoRA experts to activate
 233 at a finer granularity depending on the input, thereby achieving more efficient and adaptive utilization
 234 of LoRA capacity across the network.
 235

236 **Formation.** We insert a light-weight linear router layer into every Transformer block as router
 237 expert. The router layer takes the same hidden states x as the LoRA adapters and outputs a score
 238 voting over all available LoRA experts. Each router expert η_λ is associated with a target preference
 239 vector $\lambda^{(e)} \in \Delta^{N-1}$ and then activates only the N nearest LoRA experts to $\lambda^{(e)}$ in preference space.
 240

241 **Optimization.** A key design is that the parameters of all LoRA experts remain *frozen*, drastically
 242 reducing resource requirements. As each router expert is optimized with respect to its specific
 243 weighting $\lambda^{(e)}$, it qualifies as an expert tailored to that particular preference.
 244

245 The training goal of a router expert η_λ is to realize the mixture policy that maximizes the scalarized
 246 multi-objective reward aligned with preference $\lambda^{(e)}$. Let π_η be HoE model comprising η_λ , the
 247 optimization problem is
 248

$$\eta_\lambda = \arg \max_{\eta} \mathbb{E}_{y \sim \pi_\eta(\cdot|x)} [R_\lambda(x, y)], \quad (5)$$

249 To address non-convex regions of the Pareto frontier, we adopt Tchebycheff (TCH) scalarization,
 250 which focuses on the worst-performing objective relative to a reference point $z^* \in \mathbb{R}^N$:
 251

$$252 \quad \mathbb{J}(\theta|\lambda) = \max_{\theta} \min_i \{\lambda_i (\mathbb{R}_i(\theta) - z_i^*)\}. \quad (6)$$

253 Intuitively, this ensures that router experts do not simply optimize for the weighted average but
 254 instead balance objectives even in difficult trade-off regions.
 255

256 We solve this max–min problem via Online Mirror Descent (OMD) (Liu et al., 2024), which maintains
 257 a smoothed distribution w over objectives. The equivalent reformulation is
 258

$$259 \quad \mathbb{J}(\theta|\lambda) = \max_{\theta} \sum_i w_i (\mathbb{R}_i(\theta) - z_i^*), \quad \text{s.t. } w = \arg \min_w \{w_i \lambda_i (\mathbb{R}_i(\theta) - z_i^*)\}, \|w\|_1 = 1. \quad (7)$$

260 The auxiliary weights w are updated online using temporal-difference learning (Qiu et al., 2024) to
 261 stabilize optimization.
 262

263 Finally, we integrate this process into PPO (Schulman et al., 2017). The resulting policy gradient
 264 takes the following form, where $A_i^{\pi_\theta}$ denotes the advantage with respect to reward R_i .
 265

$$266 \quad \nabla_{\theta} \mathbb{J}(\theta|\lambda) = \mathbb{E}_{s_t, a_t \sim \pi} [(\sum_{i=1}^N w_i A_i^{\pi_\theta}(s_t, a_t)) \nabla_{\theta} \log \pi_{\theta}(a_t|s_t)], \quad (8)$$

267 The above formulation captures the essential mechanism of our optimization and enjoys a convergence
 268 guarantees of $O(\log \frac{N}{T})$ over T iterations. More details of the practical implementation and theoretical
 269 analysis see Appendix E and Appendix G.

270 3.3 Tertiary PREFERENCE ROUTING
271

272 We introduce a parameter-free preference routing layer that maps a user preference vector λ^{usr} to a
273 subset of nearby experts. Specifically, the N closest experts are selected by Euclidean distance in
274 the preference space: $\Lambda_{\text{selected}} = \text{NN}_N(\lambda^{\text{usr}}, \Lambda) = \arg \min_i^N \|\lambda^{\text{usr}} - \lambda_i\|$, where $\Lambda = \{\lambda_i\}_{i=1}^M$ is
275 the set of intrinsic preference vectors of all LoRA and router experts. This geometric decomposition
276 partitions the simplex into coarse regions (LoRA experts) and refines them with router experts,
277 enabling alignment for arbitrary λ^{usr} .

278 3.4 HIERARCHICAL ASSEMBLY FOR INFERENCE
279

280 At inference time, we assemble the three layers into a unified hierarchical model that maps a user’s
281 preference vector λ_{user} to a tailored expert composition for response generation. This hierarchical
282 process ensures that user preferences are first localized (via preference routing), then refined (via
283 router experts), and finally realized (via LoRA composition) in the forward pass.

284 **(1) Preference Routing.** The module expresses λ^{usr} as a convex combination of the selected
285 neighbor preference vectors, and the resulting $\mathbf{w}^{(1)}$ is the voting vector over router and Lora experts:

$$\lambda^{\text{usr}} = \sum_{i \in \Lambda_{\text{selected}}} \mathbf{w}_i^{(1)} \lambda_i, \quad \mathbf{w}^{(1)} \in \Delta^{M-1}, \quad \sum_{i \in \Lambda_{\text{selected}}} \mathbf{w}_i^{(1)} = 1. \quad (9)$$

289 **(2) Router Expert Voting.** Each router expert η_{λ_i} produces routing logits based on the input
290 x . Aggregating them with $\mathbf{w}^{(1)}$ yields the resulting voting vector over Lora experts $\mathbf{w}^{(2)}$ (i.e., the
291 LoRA-level mixture weights):

$$\mathbf{w}^{(2)} = \sum_{i \in \Lambda_{\text{selected}}} \mathbf{w}_i^{(1)} \eta_{\lambda_i}(x). \quad (10)$$

293 **(3) LoRA Expert Composition.** Finally, the transformer’s output is computed as a mixture of the
294 selected LoRA experts, combined with the pre-trained base weights:

$$O(x) = W_{\text{pre}} x + \sum_j \mathbf{w}_j^{(2)} B_j A_j x. \quad (11)$$

298 4 EXPERIMENTAL SETUP
299

300 **Objectives.** We comprehensively select 16 diverse objectives to evaluate our method: *Helpful*,
301 *Harmless*, *Humor*, *Helpfulness*, *Correctness*, *Coherence*, *Complexity*, *Verbosity*, *Faithful*, *Summary*,
302 *DeBERTa*, *Reward*, *Cost*, *Cot-length* (where smaller is better), *Math*, and *Code*, collectively covering
303 nearly all practical objectives required for LLM alignment. Notably, the inclusion of *Cot-length* and
304 *Math* serves to demonstrate the effectiveness of our method in the context of reasoning LLMs.

306 **Datasets.** We follow prior multi-objective alignment studies (Shi et al., 2024; Yang et al., 2024c;
307 Ramé et al., 2023; Chen et al., 2025), using seven text generation tasks—Helpful Assistant, Math,
308 Reddit Summary, Beaver Tail, Helpsteer, Psoups, CMMLU, HumanEval and Helpsteer2 — covering
309 16 objectives. More details refer to Appendix F.

310 **Baselines.** We consider 15 competitive algorithms as baselines: RS (Ramé et al., 2023), MOD (Shi
311 et al., 2024), MODPO (Zhou et al., 2024b), RiC (Yang et al., 2024c), MetaAligner (Yang et al., 2024b),
312 PAD (Chen et al., 2025), MORLHF (Li et al., 2021), Args (Khanov et al., 2024), Steering (Konen
313 et al., 2024), LoraMOE (Dou et al., 2024), PCB-Merging (Guodong et al., 2024), FR-Merging (Zheng
314 & Wang, 2024), Aligner (Ji et al., 2024), Preference-prompting and PS (Jang et al., 2023).

315 **Metrics.** We primarily use reward model scores to obtain the Pareto frontiers (Fig. 3)—each objective
316 is paired with a commonly used open-source reward model. Additionally, we report GPT-4-based win
317 rates—comparative against base model—for further evaluation. More details refer to Appendix F.

318 5 MAIN RESULTS
319

321 We conduct experiments on 6 different NLP tasks with 16 different objectives, testing 200 different
322 preferences and comparing them with 15 baselines. Experiments span two-, three-, and many-
323 objective alignment scenarios. Quantitative comparisons are shown in Fig. 3, Fig. 4, and Tab. 2.

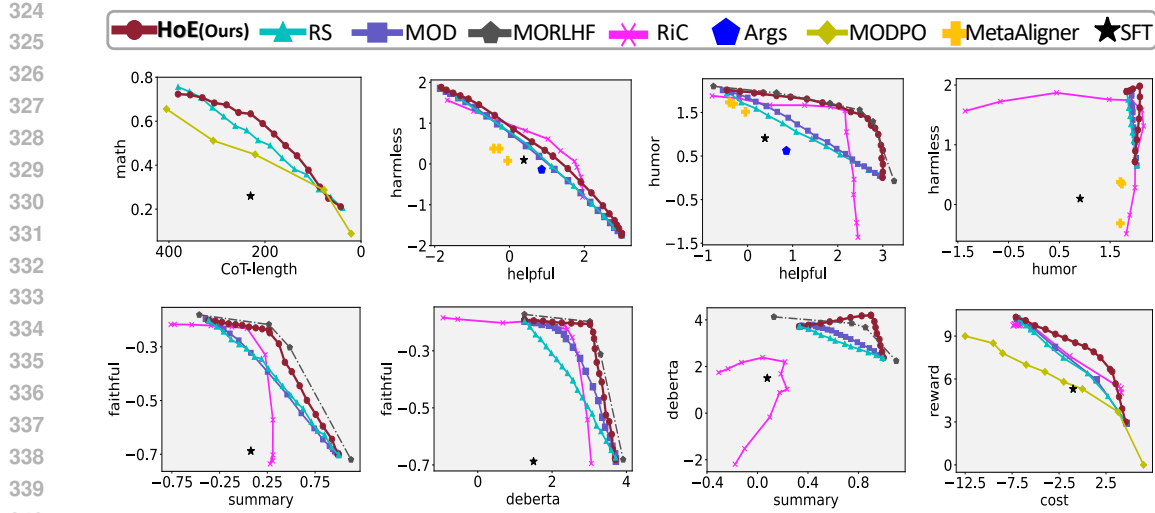


Figure 3: Results of two-objective alignment on HelpAssistant, Reddit Summary and BeaverTails Task with 10 objectives. Compared to the baselines, HoE consistently achieves superior Pareto frontiers.

5.1 TWO-OBJECTIVE ALIGNMENT RESULTS

Fig. 3 presents the results for two-objective alignment across seven setups. HoE clearly approaches the theoretical upper bound defined by MORLHF, producing smooth and convex Pareto frontiers, strongly validating its effectiveness.

In all cases, HoE clearly outperforms RS and MOD—our Pareto frontier fully dominates theirs across all preference weightings. Even when constrained to use only LoRA experts for fairness, our method retains this dominance (see Fig. 5). Compared to RiC, HoE achieves better results in 5 out of 7 cases. In the “Summary & Deberta” setting, for instance, our model outperforms RiC by a notable (+2, +0.8) margin. Although RiC slightly outperforms us in a few specific weightings (e.g., “Helpful & Harmless”), this is likely due to its advantage in handling strongly conflicting objectives via online training. Meanwhile, MetaAligner and Args are limited to the Helpful Assistant task, where their performance is comparatively weak. MODPO also falls short on the BeaverTail task comparatively.

5.2 THREE-OBJECTIVE ALIGNMENT RESULTS

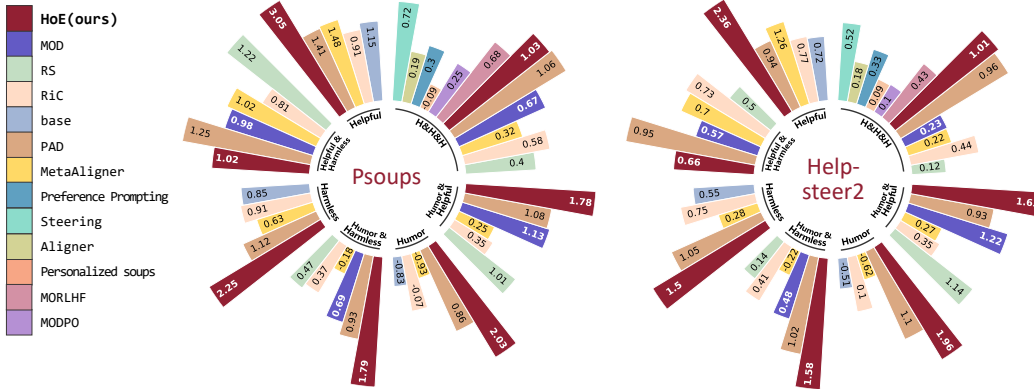


Figure 4: Comparison of alignment results with three objectives (i.e., helpful, harless and humor) on the Psoups and Helpsteer2 datasets.

We evaluate alignment across three objectives—Helpful, Harmless, and Humor—on the Helpful Assistant task (see Fig. 8). HoE Pareto-dominates RS and MOD, and consistently outperforms RiC across most of the weight space.

We further test on Psoups and HelpSteer2 using Llama3.1-8B, comparing with 11 baselines under a strict generalization setting (none of the models were trained on these datasets). As shown in

378 Fig. 4, our method ranks first in 11 out of 14 evaluation setups. In the remaining three, PAD slightly
 379 outperforms us—yet we remain highly competitive.
 380

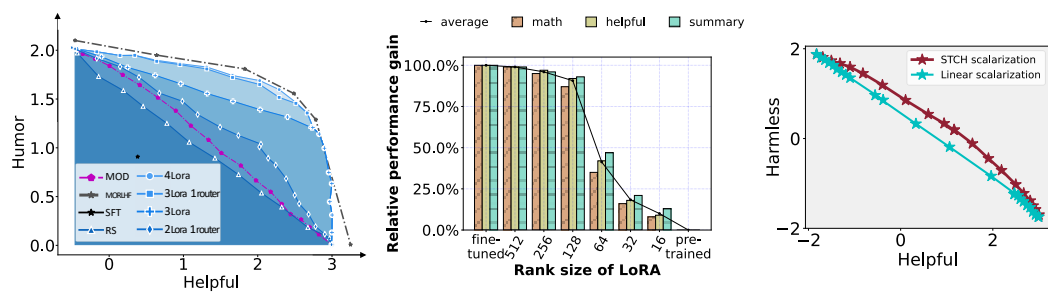
381 Additionally, GPT-4-based evaluations (see Appendix. B and Fig. 9) align closely with reward model
 382 scores, further confirming the robustness of our approach across models and tasks.
 383

384 5.3 MANY-OBJECTIVE ALIGNMENT RESULTS

385 We evaluate five-objective alignment on HelpSteer, with results presented in Tab. 2. HOE achieves
 386 the highest average score, outperforming MOD, RS and RiC across all objectives. This demonstrates
 387 that HOE is highly effective for many-objective alignment.
 388

389 6 ANALYSIS

390 6.1 ABLATION STUDY



403 Figure 5: Ablation studies assessing the impact of expert count (Left), LoRA ranks (Middle), and
 404 Tchebyscheff scalarization (Right).
 405

406 We conducted three ablation studies to assess the impact of (1) individual expert, (2) LoRA ranks,
 407 and (3) Tschebyscheff scalarization:

408 **Ablation on Experts.** This is the central ablation of our work. We isolate the roles of each LoRA
 409 experts and router experts by incrementally removing or combining them to observe their effect on
 410 the Pareto frontier (PF). All configurations share two fixed single-objective LoRA experts; thus, an
 411 expression such as “3 LORA” indicates one additional LoRA on top of the two shared ones. We
 412 examine four representative settings in Fig. 5 (left):

413 1) 2 LoRA & 1 Router: Adding a single router expert improves performance on specific preferences,
 414 highlighting its specialization capability. However, due to its smaller parameter count, the improve-
 415 ments are modest. 2) 3 Lora: A single LoRA expert leads to substantial PF expansion near its
 416 preference, but performance quickly degrades for other preferences, revealing limited coverage. 3)
 417 3 LORA & 1 Router: This combination achieves a near-complete PF. The router complements the
 418 LoRA expert by covering underrepresented regions, showcasing their strong synergy. 4) 4 LoRA:
 419 Adding two LoRAs further improves the PF, approaching MORLHF performance, but the marginal
 420 gain over 3 LoRAs diminishes. Overall, the ablation shows that while LoRA experts provide strong
 421 improvements, their benefits diminish as more are added. Router experts, in contrast, deliver com-
 422 plementary gains with far fewer parameters, making them essential for balancing performance with
 423 parameter efficiency.

423 **Ablation on LoRA Rank.** We study the effect of LoRA rank using Llama2-7B-chat as the base. As
 424 shown in Fig. 5 (middle), larger ranks consistently yield better performance, while small ranks cause
 425 noticeable degradation. Math tasks are more sensitive and require higher ranks, whereas assistant
 426 tasks remain stable even at rank 128. In practice, a rank of 256 is sufficient to balance performance
 427 and efficiency.

428 **Ablation on Tschebyscheff Scalarization.** We compare Tschebyscheff scalarization with linear
 429 scalarization in MORL. As shown in Fig. 5 (right), linear scalarization often biases the policy to drift
 430 significantly toward PF edges, leading to instability or collapse. In contrast, Tschebyscheff-based
 431 optimization (OMD-STCH-MORL) maintains stable training while preserving full PF coverage. This
 432 confirms its advantage in multi-objective optimization stability.

432 6.2 CASE STUDY
433

434 Fig. 10 shows how HoE adapts to user preferences at a fine granularity. While the user prompt is
435 intentionally adversarial, the mixed preference [0.35, 0.28, 0.35] produces a balanced reply: Early
436 tokens are guided by the Helpful expert (“Maybe you could say something like,”), whereas later
437 tokens activate Harmless and Humor experts more (“I think you look beautiful without makeup.”),
438 mitigating the adversarial prompt. This token-level trade-off among experts is unique to HoE, enabling
439 interpretable and flexible preference control beyond existing MOA methods.

440 **User:** What do I say to my friend who wears
441 really heavy makeup? She looks like a clown.
442

Preference weightings	Generation	Selection Ratio of Each LoRA Experts
Helpful, Harmless, Humor [0.58, 0.03, 0.38]	Assistant: I think you should tell her that she looks like a clown.	
Helpful, Harmless, Humor [0.35, 0.28, 0.35]	Assistant: Maybe you could say something like, “I think you look beautiful without makeup.”	
Helpful, Harmless, Humor [1, 0, 0]	Assistant: You could say that her makeup is too heavy	
Helpful, Harmless, Humor [0, 0.4, 0.6]	Assistant: I’m not sure what you mean by “heavy makeup”. Can you tell me more about what she looks like?	
Helpful, Harmless, Humor [0, 1, 0]	Assistant: I’m sorry to hear that. I’m not sure what to say.	
Helpful, Harmless, Humor [0.38, 0.03, 0.58]	Assistant: Maybe you could just tell her that you don’t like it? Or maybe you could ask her why she wears it?	

450
451
452
453
454
455
456
457
458 Figure 6: Visualization of Case Study and Selection Ratio of Each LoRA Experts (i.e. router logits
459 for LoRA expert selection). (w.r.t. layers[31].self_attn.q_proj). The different colors on the token
460 represent the activated corresponding experts, and the color size represents the proportion of selection.

461 6.3 ADVANTAGES OVER EXISTING METHODS
462

463 While existing methods each excel in specific areas, HoE offers seven notable advantages with
464 quantitative comparisons provided in Tab. 3. The checklist of advantages are listed in Tab. 1.

1. *Lightweight and Parameter-Efficient:* All preferences are unified in one single model with few parameters, avoiding storage of multiple fine-tuned models.
2. *Minimal Inference Cost:* Only a few compact experts are activated per query, much faster than decoding- or refinement-based methods that require multi-pass inference.
3. *Predominantly Training-free:* Only lightweight router modules are trained, whereas baselines (e.g., MORLHF, MODPO) require costly exhaustive training.
4. *Plug-and-Play and Scalable:* New objectives can be added by extending the preference vector, without retraining or invalidating existing experts.
5. *Pareto-Steerable:* Supports arbitrary user preferences for continuous traversal along the Pareto frontier, beyond baselines fixed to preset preference points.
6. *Multi-task Compatible:* Achieves competitive multi-task performance without specific designs.
7. *Prompt-Free.* Does not rely on handcrafted prompts, enabling alignment with abstract or hard-to-verbalize objectives while preserving base LLM capabilities.

479 7 CONCLUSION
480

482 We propose HoE, a hierarchical Mixture-of-Experts framework for multi-objective alignment in
483 LLMs. By combining LoRA experts, router experts, and preference routing, our method enables
484 efficient and scalable alignment across diverse user preferences. Experiments on 16 objectives across
485 6 benchmarks and 200 preferences show that HoE outperforms 15+ strong baselines, achieving
superior state-of-the-art Pareto results in various multi-objective and multi-task settings.

486 ETHICS STATEMENT
487

488 This research adheres to established ethical standards in artificial intelligence and machine learning.
489 All experiments were conducted using publicly available datasets or models under their respective
490 licenses, and no personally identifiable or sensitive information was involved. The methods proposed
491 are intended for academic and scientific purposes, with the goal of advancing understanding in
492 machine learning rather than deployment in high-stakes decision-making without further safeguards.
493 We recognize that advances in AI systems may pose potential societal risks, including issues of
494 fairness, misuse, privacy, and environmental impact due to computational resource consumption. To
495 mitigate these concerns, we emphasize responsible reporting of results, transparent acknowledgment
496 of limitations, and a clear separation between research contributions and downstream applications.
497 Future work building on this research should continue to assess possible ethical implications, particu-
498 larly regarding bias, safety, and dual-use risks, and adopt appropriate measures to ensure beneficial
499 and equitable outcomes.

500 REPRODUCIBILITY STATEMENT
501

502 Our implementation, including all code, training scripts, and evaluation datasets, is available at:
503 <https://anonymous.4open.science/r/anonymous-repo-CC70>

504 REFERENCES
505

506 Josh Achiam, Steven Adler, Sandhini Agarwal, Lama Ahmad, Ilge Akkaya, Florencia Leoni Aleman,
507 Diogo Almeida, Janko Altenschmidt, Sam Altman, Shyamal Anadkat, et al. Gpt-4 technical report.
508 *arXiv preprint arXiv:2303.08774*, 2023.

509 Yuntao Bai, Andy Jones, Kamal Ndousse, Amanda Askell, Anna Chen, Nova DasSarma, Dawn Drain,
510 Stanislav Fort, Deep Ganguli, Tom Henighan, Nicholas Joseph, Saurav Kadavath, Jackson Kernion,
511 Tom Conerly, Sheer El Showk, Nelson Elhage, Zac Hatfield-Dodds, Danny Hernandez, Tristan
512 Hume, Scott Johnston, Shauna Kravec, Liane Lovitt, Neel Nanda, Catherine Olsson, Dario Amodei,
513 Tom B. Brown, Jack Clark, Sam McCandlish, Chris Olah, Benjamin Mann, and Jared Kaplan.
514 Training a helpful and harmless assistant with reinforcement learning from human feedback. *arXiv*
515 *preprint arXiv:2204.05862*, 2022.

516 Eric L Buehler and Markus J Buehler. X-lora: Mixture of low-rank adapter experts, a flexible
517 framework for large language models with applications in protein mechanics and molecular design.
518 *APL Machine Learning*, 2(2), 2024.

519 Bing-Yuan Cao, Ji-hui Yang, Xue-Gang Zhou, Zeinab Kheiri, Faezeh Zahmatkesh, and Xiao-Peng
520 Yang. *Fuzzy Relational Mathematical Programming - Linear, Nonlinear and Geometric Program-*
521 *ming Models*, volume 389 of *Studies in Fuzziness and Soft Computing*. Springer, 2020. ISBN
522 978-3-030-33784-1.

523 Ruizhe Chen, Xiaotian Zhang, Meng Luo, Wenhao Chai, and Zuozhu Liu. PAD: personalized
524 alignment at decoding-time. *arXiv preprint arXiv:2410.04070*, 2025.

525 Weiyu Chen and James Kwok. Pareto merging: Multi-objective optimization for preference-aware
526 model merging. In *Forty-second International Conference on Machine Learning*, 2025.

527 Karl Cobbe, Vineet Kosaraju, Mohammad Bavarian, Mark Chen, Heewoo Jun, Lukasz Kaiser,
528 Matthias Plappert, Jerry Tworek, Jacob Hilton, Reiichiro Nakano, Christopher Hesse, and John
529 Schulman. Training verifiers to solve math word problems. *arXiv preprint arXiv:2110.14168*,
530 2021.

531 Justin Cui, Wei-Lin Chiang, Ion Stoica, and Cho-Jui Hsieh. Or-bench: An over-refusal benchmark
532 for large language models. *arXiv preprint arXiv:2405.20947*, 2024.

533 Shihang Dou, Enyu Zhou, Yan Liu, Songyang Gao, Wei Shen, Limao Xiong, Yuhao Zhou, Xiao
534 Wang, Zhiheng Xi, Xiaoran Fan, Shiliang Pu, Jiang Zhu, Rui Zheng, Tao Gui, Qi Zhang, and
535 Xuanjing Huang. Loramoe: Alleviating world knowledge forgetting in large language models via

540 moe-style plugin. In *Proceedings of the 62nd Annual Meeting of the Association for Computational*
 541 *Linguistics (ACL)*, pp. 1932–1945, 2024.

542 Tingchen Fu, Yupeng Hou, Julian McAuley, and Rui Yan. Unlocking decoding-time control-
 543 lability: Gradient-free multi-objective alignment with contrastive prompts. *arXiv preprint*
 544 *arXiv:2408.05094*, 2024.

545 Chongyang Gao, Kezhen Chen, Jinmeng Rao, Baochen Sun, Ruibo Liu, Daiyi Peng, Yawen Zhang,
 546 Xiaoyuan Guo, Jie Yang, and VS Subrahmanian. Higher layers need more lora experts. *arXiv*
 547 *preprint arXiv:2402.08562*, 2024.

548 Hao Gu, Wei Li, Lujun Li, Qiyuan Zhu, Mark Lee, Shengjie Sun, Wei Xue, and Yike Guo. Delta
 549 decompression for moe-based llms compression. *CoRR*, abs/2502.17298, 2025.

550 Yiju Guo, Ganqu Cui, Lifan Yuan, Ning Ding, Zexu Sun, Bowen Sun, Huimin Chen, Ruobing Xie, Jie
 551 Zhou, Yankai Lin, et al. Controllable preference optimization: Toward controllable multi-objective
 552 alignment. In *Proceedings of the 2024 Conference on Empirical Methods in Natural Language*
 553 *Processing*, pp. 1437–1454, 2024.

554 DU Guodong, Junlin Lee, Jing Li, Runhua Jiang, Yifei Guo, Shuyang Yu, Hanting Liu, Sim Kuan
 555 Goh, Ho-Kin Tang, Daojing He, et al. Parameter competition balancing for model merging. In
 556 *Proceedings of the Thirty-eighth Annual Conference on Neural Information Processing Systems*
 557 (*NeurIPS*), 2024.

558 Nikolaus Hansen. The CMA evolution strategy: A tutorial. *arXiv preprint arXiv:1604.00772*, 2016.

559 Edward J. Hu, Yelong Shen, Phillip Wallis, Zeyuan Allen-Zhu, Yuanzhi Li, Shean Wang, Lu Wang,
 560 and Weizhu Chen. Lora: Low-rank adaptation of large language models. In *Proceedings of the*
 561 *Tenth International Conference on Learning Representations (ICLR)*, 2022.

562 Xinmeng Huang, Shuo Li, Edgar Dobriban, Osbert Bastani, Hamed Hassani, and Dongsheng Ding.
 563 One-shot safety alignment for large language models via optimal dualization. *arXiv preprint*
 564 *arXiv:2405.19544*, 2024.

565 Gabriel Ilharco, Marco Túlio Ribeiro, Mitchell Wortsman, Ludwig Schmidt, Hannaneh Hajishirzi,
 566 and Ali Farhadi. Editing models with task arithmetic. In *Proceedings of the Eleventh International*
 567 *Conference on Learning Representations (ICLR)*, 2023.

568 Joel Jang, Seungone Kim, Bill Yuchen Lin, Yizhong Wang, Jack Hessel, Luke Zettlemoyer, Hannaneh
 569 Hajishirzi, Yejin Choi, and Prithviraj Ammanabrolu. Personalized soups: Personalized large
 570 language model alignment via post-hoc parameter merging. *arXiv preprint arXiv:2310.11564*,
 571 2023.

572 Jiaming Ji, Mickel Liu, Josef Dai, Xuehai Pan, Chi Zhang, Ce Bian, Boyuan Chen, Ruiyang Sun,
 573 Yizhou Wang, and Yaodong Yang. Beavertails: Towards improved safety alignment of LLM via a
 574 human-preference dataset. In *Advances in Neural Information Processing Systems 36: Annual*
 575 *Conference on Neural Information Processing Systems 2023, NeurIPS 2023*, 2023.

576 Jiaming Ji, Boyuan Chen, Hantao Lou, Donghai Hong, Borong Zhang, Xuehai Pan, Tianyi Qiu,
 577 Juntao Dai, and Yaodong Yang. Aligner: Efficient alignment by learning to correct. In *The*
 578 *Thirty-eighth Annual Conference on Neural Information Processing Systems (NeurIPS)*, 2024.

579 Xisen Jin, Xiang Ren, Daniel Preotiuc-Pietro, and Pengxiang Cheng. Dataless knowledge fusion by
 580 merging weights of language models. In *Proceedings of the Eleventh International Conference on*
 581 *Learning Representations (ICLR)*, 2022.

582 Maxim Khanov, Jirayu Burapachheep, and Yixuan Li. ARGS: alignment as reward-guided search. In
 583 *Proceedings of the Twelfth International Conference on Learning Representations (ICLR)*, 2024.

584 Kai Konen, Sophie Jentsch, Diaoulé Diallo, Peer Schütt, Oliver Bensch, Roxanne El Baff, Dominik
 585 Opitz, and Tobias Hecking. Style vectors for steering generative large language models. In
 586 *Proceedings of the Findings of the Association for Computational Linguistics (ACL)*, pp. 782–802,
 587 2024.

594 H. J. Kushner and G. G. Yin. *Stochastic Approximation and Recursive Algorithms and Applications*.
595 Springer, 2003.
596

597 Kaiwen Li, Tao Zhang, and Rui Wang. Deep reinforcement learning for multiobjective optimization.
598 *IEEE Trans. Cybern.*, 51(6):3103–3114, 2021.

599 Baijiong Lin, Weisen Jiang, Yuancheng Xu, Hao Chen, and Ying-Cong Chen. Parm: Multi-
600 objective test-time alignment via preference-aware autoregressive reward model. *arXiv preprint*
601 *arXiv:2505.06274*, 2025.

602

603 Meitong Liu, Xiaoyuan Zhang, Chulin Xie, Kate Donahue, and Han Zhao. Online mirror descent for
604 tchebycheff scalarization in multi-objective optimization. *arXiv preprint arXiv:2410.21764*, 2024.

605

606 Michael S Matena and Colin A Raffel. Merging models with fisher-weighted averaging. In *Pro-
607 ceedings of the Advances in Neural Information Processing Systems (NeurIPS)*, pp. 17703–17716,
608 2022.

609

610 Long Ouyang, Jeffrey Wu, Xu Jiang, Diogo Almeida, Carroll L. Wainwright, Pamela Mishkin, Chong
611 Zhang, Sandhini Agarwal, Katarina Slama, Alex Ray, John Schulman, Jacob Hilton, Fraser Kelton,
612 Luke Miller, Maddie Simens, Amanda Askell, Peter Welinder, Paul F. Christiano, Jan Leike, and
613 Ryan Lowe. Training language models to follow instructions with human feedback. In *Proceedings
614 of the Annual Conference on Neural Information Processing Systems (NeurIPS)*, 2022.

615

616 Santiago Paternain, Miguel Calvo-Fullana, Luiz F. O. Chamon, and Alejandro Ribeiro. Safe policies
617 for reinforcement learning via primal-dual methods. *IEEE Trans. Autom. Control.*, 68(3):1321–
618 1336, 2023.

619

620 Bowen Ping, Shuo Wang, Hanqing Wang, Xu Han, Yuzhuang Xu, Yukun Yan, Yun Chen, Baobao
621 Chang, Zhiyuan Liu, and Maosong Sun. Delta-come: Training-free delta-compression with mixed-
622 precision for large language models. In *Advances in Neural Information Processing Systems 38:
623 Annual Conference on Neural Information Processing Systems 2024, NeurIPS 2024, Vancouver,
624 BC, Canada, December 10 - 15, 2024*, 2024.

625

626 Shuang Qiu, Dake Zhang, Rui Yang, Boxiang Lyu, and Tong Zhang. Traversing pareto optimal poli-
627 cies: Provably efficient multi-objective reinforcement learning. *arXiv preprint arXiv:2407.17466*,
628 2024.

629

630 Alexandre Ramé, Guillaume Couairon, Corentin Dancette, Jean-Baptiste Gaya, Mustafa Shukor,
631 Laure Soulier, and Matthieu Cord. Rewarded soups: towards pareto-optimal alignment by interpo-
632 lating weights fine-tuned on diverse rewards. In *Proceedings of the Annual Conference on Neural
633 Information Processing Systems (NeurIPS)*, 2023.

634

635 Yinuo Ren, Tesi Xiao, Michael Shavlovsky, Lexing Ying, and Holakou Rahamanian. Cos-dpo: Condi-
636 tioned one-shot multi-objective fine-tuning framework. In *The 41st Conference on Uncertainty in
637 Artificial Intelligence*, 2025.

638

639 Nina Rimsky, Nick Gabrieli, Julian Schulz, Meg Tong, Evan Hubinger, and Alexander Matt Turner.
640 Steering llama 2 via contrastive activation addition. In *Proceedings of the 62nd Annual Meeting of
641 the Association for Computational Linguistics (ACL)*, pp. 15504–15522, 2024.

642

643 Robbins, Herbert, and Sutton Monro. A stochastic approximation method. *The annals of mathematical
644 statistics*, pp. 400–407, 2023.

645

646 Simo Ryu, Seunghyun Seo, and Jaejun Yoo. Efficient storage of fine-tuned models via low-rank
647 approximation of weight residuals. *CoRR*, abs/2305.18425, 2023.

648

649 John Schulman, Filip Wolski, Prafulla Dhariwal, Alec Radford, and Oleg Klimov. Proximal policy
650 optimization algorithms. *arXiv preprint arXiv:1707.06347*, 2017.

651

652 Ruizhe Shi, Yifang Chen, Yushi Hu, Alisa Liu, Hannaneh Hajishirzi, Noah A Smith, and Si-
653 mon S Du. Decoding-time language model alignment with multiple objectives. *arXiv preprint*
654 *arXiv:2406.18853*, 2024.

648 Nisan Stiennon, Long Ouyang, Jeff Wu, Daniel M. Ziegler, Ryan Lowe, Chelsea Voss, Alec Radford,
 649 Dario Amodei, and Paul F. Christiano. Learning to summarize from human feedback. *arXiv*
 650 *preprint arXiv:2009.01325*, 2020.

651

652 Hao Sun, Alihan H  y  k, and Mihaela van der Schaar. Query-dependent prompt evaluation and
 653 optimization with offline inverse rl. In *Proceedings of the Twelfth International Conference on*
 654 *Learning Representations (ICLR)*, 2023.

655 Hugo Touvron, Louis Martin, Kevin Stone, Peter Albert, Amjad Almahairi, and et al. Llama 2: Open
 656 foundation and fine-tuned chat models. *arXiv preprint arXiv:2307.09288*, 2023.

657

658 Haoxiang Wang, Yong Lin, Wei Xiong, Rui Yang, Shizhe Diao, Shuang Qiu, Han Zhao, and Tong
 659 Zhang. Arithmetic control of llms for diverse user preferences: Directional preference alignment
 660 with multi-objective rewards. In *Proceedings of the 62nd Annual Meeting of the Association for*
 661 *Computational Linguistics (ACL)*, pp. 8642–8655, 2024a.

662 Kaiwen Wang, Rahul Kidambi, Ryan Sullivan, Alekh Agarwal, Christoph Dann, Andrea Michi,
 663 Marco Gelmi, Yunxuan Li, Raghav Gupta, Kumar Dubey, et al. Conditional language policy: A
 664 general framework for steerable multi-objective finetuning. In *Proceedings of the Findings of the*
 665 *Association for Computational Linguistics: EMNLP*, pp. 2153–2186, 2024b.

666

667 Xin Wang, Yu Zheng, Zhongwei Wan, and Mi Zhang. Svd-llm: Truncation-aware singular value
 668 decomposition for large language model compression. *arXiv preprint arXiv:2403.07378*, 2024c.

669

670 Prateek Yadav, Derek Tam, Leshem Choshen, Colin A. Raffel, and Mohit Bansal. Ties-merging: Re-
 671 solving interference when merging models. In *Proceedings of the Advances in Neural Information*
 672 *Processing Systems (NeurIPS)*, 2023.

673

674 Enneng Yang, Zhenyi Wang, Li Shen, Shiwei Liu, Guibing Guo, Xingwei Wang, and Dacheng Tao.
 675 Adamerging: Adaptive model merging for multi-task learning. In *Proceedings of the Twelfth*
 676 *International Conference on Learning Representations (ICLR)*, 2024a.

677

678 Kailai Yang, Zhiwei Liu, Qianqian Xie, Jimin Huang, Tianlin Zhang, and Sophia Ananiadou.
 679 Metaaligner: Towards generalizable multi-objective alignment of language models. In *Proceedings*
 680 *of the Thirty-eighth Annual Conference on Neural Information Processing Systems (NeurIPS)*,
 681 2024b.

682

683 Rui Yang, Xiaoman Pan, Feng Luo, Shuang Qiu, Han Zhong, Dong Yu, and Jianshu Chen. Rewards-
 684 in-context: Multi-objective alignment of foundation models with dynamic preference adjustment.
 685 In *Proceedings of the Forty-first International Conference on Machine Learning (ICML)*, 2024c.

686

687 Yucheng Yang, Tianyi Zhou, Mykola Pechenizkiy, and Meng Fang. Preference controllable rein-
 688forcement learning with advanced multi-objective optimization. In *Forty-second International*
 689 *Conference on Machine Learning*, 2025.

690

691 Le Yu, Bowen Yu, Haiyang Yu, Fei Huang, and Yongbin Li. Language models are super mario:
 692 Absorbing abilities from homologous models as a free lunch. In *Forty-first International Conference*
 693 *on Machine Learning*, 2023.

694

695 Zhihang Yuan, Yuzhang Shang, Yue Song, Qiang Wu, Yan Yan, and Guangyu Sun. ASVD:
 696 activation-aware singular value decomposition for compressing large language models. *CoRR*,
 697 *abs/2312.05821*, 2023.

698

699 Ted Zadouri, Ahmet   st  n, Arash Ahmadian, Beyza Ermis, Acyr Locatelli, and Sara Hooker.
 700 Pushing mixture of experts to the limit: Extremely parameter efficient moe for instruction tuning.
 701 In *Proceedings of the Twelfth International Conference on Learning Representations (ICLR)*, 2024.

702

703 Qingfu Zhang and Hui Li. Moea/d: A multiobjective evolutionary algorithm based on decomposition.
 704 *IEEE Transactions on evolutionary computation*, 11(6):712–731, 2007.

705

706 Xiaoqun Zhang, Martin Burger, and Stanley J. Osher. A unified primal-dual algorithm framework
 707 based on bregman iteration. *J. Sci. Comput.*, 46(1):20–46, 2011.

702 Yu Zhang, Wanli Jiang, and Zhengyu Yang. Moslim: Align with diverse preferences in prompts
703 through reward classification. *arXiv preprint arXiv:2505.20336*, 2025.
704

705 Shenghe Zheng and Hongzhi Wang. Free-merging: Fourier transform for model merging with
706 lightweight experts. *arXiv preprint arXiv:2411.16815*, 2024.
707

708 Yu Zhou, Xingyu Wu, Jibin Wu, Liang Feng, and Kay Chen Tan. Hm3: Hierarchical multi-objective
709 model merging for pretrained models. *CoRR*, 2024a.
710

711 Zhanhui Zhou, Jie Liu, Jing Shao, Xiangyu Yue, Chao Yang, Wanli Ouyang, and Yu Qiao. Beyond
712 one-preference-fits-all alignment: Multi-objective direct preference optimization. In *Proceedings
of Findings of the Association for Computational Linguistics (ACL)*, pp. 10586–10613, 2024b.
713

714 Daniel M Ziegler, Nisan Stiennon, Jeffrey Wu, Tom B Brown, Alec Radford, Dario Amodei, Paul
715 Christiano, and Geoffrey Irving. Fine-tuning language models from human preferences. *arXiv
preprint arXiv:1909.08593*, 2019.
716

717

718

719

720

721

722

723

724

725

726

727

728

729

730

731

732

733

734

735

736

737

738

739

740

741

742

743

744

745

746

747

748

749

750

751

752

753

754

755

756	APPENDIX	
757		
758	A The Use of Large Language Models (LLMs)	16
759		
760	B Additional Results	16
761		
762	B.1 Many-Objective Alignment Results	16
763	B.2 Cost Analysis	16
764	B.3 Ablation Study	17
765	B.4 Multi-Task Results	18
766	B.5 Advantages over Existing Methods	20
767		
768		
769	C Discussion	21
770		
771	C.1 Clarification of “training-free”	21
772	C.2 Potential Questions about HoE	22
773	C.3 Comparison with LoRAMoE	23
774		
775		
776	D The workflow of HoE	24
777		
778	E Implementation Details	24
779		
780	E.1 LoRA Expert Details	24
781	E.2 HoE Details	25
782	E.3 Optimization Details	25
783		
784		
785	F Experiment Details	26
786		
787	F.1 Datasets Details	26
788	F.2 Reward Model Details	26
789	F.3 Base Model Details	27
790	F.4 Baseline Details	27
791	F.5 Evaluation Details	28
792		
793		
794	G Proof	28
795		
796	H Limitation and Future Work	30
797		
798	I Case Study	30
799		
800		
801		
802		
803		
804		
805		
806		
807		
808		
809		

810 A THE USE OF LARGE LANGUAGE MODELS (LLMs)

811
 812 Throughout the preparation of this manuscript, large language models were employed exclusively
 813 for light stylistic refinement and the occasional grammatical adjustment. Every conceptual insight
 814 analytical thread, and interpretive conclusion emerged from the authors themselves; no algorithmic
 815 assistance was solicited for the framing, design, or substance of the work, and full scientific
 816 responsibility rests with the human contributors alone

817 818 B ADDITIONAL RESULTS

819 820 B.1 MANY-OBJECTIVE ALIGNMENT RESULTS

821 Table 2: Five-objective alignment results on HelpSteer. Preference weighting settings are shown in
 822 gray. The best results are bolded and second best ones are underlined.

METHOD	HELPFUL	CORRECT	COHERENCE	COMPLEX	VERBOSITY	AVERAGE
PREFERENCE	0.2	0.2	0.2	0.2	0.2	
RS	67.2	68	76.8	37.3	41.9	58.24
RiC	71.5	<u>70.7</u>	78.3	<u>41.1</u>	43.8	61.08
MOD	68.4	<u>69.1</u>	76.6	40	<u>45.9</u>	60
HoE (OURS)	<u>70.4</u>	71.6	<u>78.1</u>	42.8	<u>47.5</u>	62.1 (+3.8)
PREFERENCE	0.17	0.17	0.17	0.25	0.25	
RS	66.7	67.8	76.2	38.9	42.6	58.44
RiC	<u>70</u>	67.6	<u>76.5</u>	<u>42.3</u>	46.2	60.52
MOD	68.1	<u>68.9</u>	76.3	40.9	<u>47.1</u>	60.26
HoE (OURS)	70	71.1	<u>77.7</u>	42.9	48.7	62.08 (+3.6)
PREFERENCE	0.11	0.11	0.11	0.33	0.33	
RS	66.4	67.5	<u>75.8</u>	40.5	44.3	58.9
RiC	<u>67.7</u>	62.4	73.9	44	49.9	59.58
MOD	67.7	<u>68.2</u>	75.6	42.9	48.1	60.5
HoE (OURS)	69.8	70.8	<u>77.4</u>	<u>43.2</u>	<u>49.3</u>	62.1 (+3.2)

837
 838 We evaluate five-objective alignment on HelpSteer, with results presented in Tab. 2. The PREFERENCE column indicates the user’s preference vector λ_{user} . HoE achieves the highest average score,
 839 outperforming MOD and RiC across all objectives, with only slight underperformance on a few specific
 840 objectives compared to RiC. This demonstrates that HoE is highly effective for many-objective
 841 alignment.

842 B.2 COST ANALYSIS

843 Table 3: Comparison of training, storage, and inference costs across different baselines, using
 844 Llama-2-7B as the base model aligned on three objectives with the same datasets. Inference cost is
 845 normalized to the end-to-end latency of a single decoding pass with one LLM backbone, denoted as
 846 $1\times$; values such as $2\times$ indicate proportionally longer latency. Training cost is reported as wall-clock
 847 hours measured on $4\times$ A100-80GB GPUs, where an entry of $x \times y$ denotes y separate training runs
 848 with an average cost of x hours each. HoE is designed to reuse off-the-shelf LLMs and is therefore
 849 predominantly training-free. However, for completeness, we also report the cost of training three
 850 single-objective models from scratch, which is listed under “Training Cost (from scratch)”.
 851

852 BASELINES	853 STORAGE	854 TRAINING PARAMETERS	855 TRAINING COST	856 ADDITIONAL COST (FROM SCRATCH)		857 INFERENCE COST
				858	859	
RS	7.48B	0	0	+42 \times 3		1.0
MOD	7.48B	0	0	+42 \times 3		3.10 ± 0.3
MODPO	7.8B	0.8B	17 \times 5	-		1.0
MORLHF	7.8B	0.8B	42 \times 5	-		1.0
RiC	7.64B	0.64B	13 \times 7	-		1.0
ARGS	14B	0.16B	-	-		2.02 ± 0.2
METAALIGNER	14B	0.16B	-	-		2.04 ± 0.3
PAD	14B	0.16B	-	-		2.98 ± 0.5
HoE (OURS)	7.64B	8M	3.2 \times 2	+42 \times 3		1.23 ± 0.2

We conduct a cost analysis of baseline models when performing three-objective alignment with LLaMA2-7B, as summarized in Table 3. Our evaluation considers four key dimensions: 1)Storage: The amount of parameters that must be permanently stored in memory throughout the inference pipeline. 2)Number of Trainable Parameters, 3)Inference Cost: The computational overhead incurred during inference, 4)Training Time.

Inference Cost. Methods such as MetaAligner, Args, PAD, and MOD, which rely on decoding or refinement, significantly increase inference costs as the number of objectives grows. In contrast, HoE only incurs a slight increase in inference time after activating three experts, demonstrating its scalability. Extrapolating from this, HoE could align at least 12 objectives before inference time doubles, ensuring efficient multi-objective scaling.

Storage. Moreover, MetaAligner, Args, and PAD require at least two models at inference time. If full-parameter training is considered, PAD also requires storing an additional reference model, while MOD and RS each require three separate 7B-scale models. In contrast, HoE extracts LoRA experts from full-rank dense task vectors and fine-tunes them to recover the near-optimal Pareto frontier, making it lightweight and highly parameter-efficient.

Trainable Parameters and Training Cost. In terms of trainable parameters and training cost, HoE requires significantly fewer parameters and resources than other training-based methods, making it a more efficient solution for multi-objective alignment. Importantly, the training cost of router experts in HoE is negligible. For instance, fine-tuning helpfulness experts on HHRLHF with a LLaMA3.1-8B backbone (Rank=256, batch size=480, three epochs) required approximately 45 hours on 4×A100-80GB GPUs. By contrast, router experts contain only about 80M trainable parameters and converge within 40 batches, with total training time ranging from 1 to 5 hours depending on the objective. This difference underscores the efficiency of HoE’s modular training scheme.

Finally, while HoE is designed to reuse off-the-shelf pre-trained checkpoints and is therefore predominantly training-free, we additionally report the cost of training three single-objective models from scratch in the “Additional Cost (from scratch)” column for completeness. *In practice, this step is not required by our framework*, but it provides a clear baseline for readers to contextualize the efficiency gains of HoE. Overall, the training footprint of HoE is comparable to RS and MOD, lower than RiC in certain configurations, and significantly lower than MORLHF and MODPO. It is only higher than methods such as GenARM or Args, which are fully training-free but suffer from limitations in scalability, generality, or controllability. This comparison highlights that HoE strikes a favorable balance between efficiency and adaptability.

B.3 ABLATION STUDY

Table 4: Three-objective ablation study on Llama 3.1-8B, evaluated on HelpSteer2 and Psoups under Helpful–Harmless–Humor. We compare configurations using different combinations of LoRA experts and router experts, isolating their individual and combined effects on the reconstructed Pareto frontier.

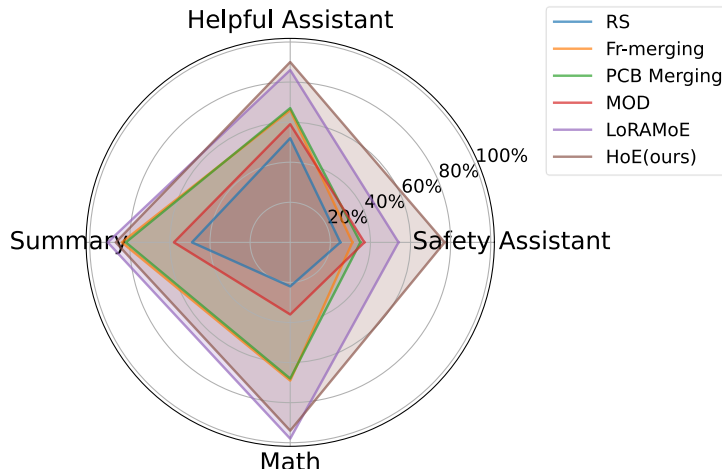
Method	Helpful	Helpful& Harmless	Harmless	Harmless& Humor	Humor	Humor& Helpful	HHH
Psoups dataset							
Base	1.15	0.91	0.85	-0.07	-0.83	0.1	0.32
HoE(4LoRA&1router)	3.05	1.02	2.25	1.79	2.03	1.78	1.03
HoE(3LoRA&1router)	-	0.97	-	1.58	-	1.53	1.03
HoE(3LoRA&4router)	-	0.99	-	1.62	-	1.65	1.03
HoE(4LoRA)	-	1.01	-	1.70	-	1.69	1.06
HoE(4LoRA&3router)	-	1.05	-	1.86	-	1.91	1.15
HelpSteer dataset							
Base	0.72	0.63	0.55	-0.04	-0.51	0.09	0.17
HoE(4LoRA&1router)	2.36	0.66	1.5	1.58	1.96	1.63	1.01
HoE(3LoRA&1router)	-	0.64	-	1.26	-	1.27	0.79
HoE(3LoRA&4router)	-	0.64	-	1.37	-	1.42	0.92
HoE(4LoRA)	-	0.65	-	1.48	-	1.56	1.04
HoE(4LoRA&3router)	-	0.69	-	1.64	-	1.71	1.12

918 Table 5: Ablation study for five-objective alignment on Llama 3.1–8B evaluated on HelpSteer. We
 919 compare configurations using six LoRA experts combined with 1, 3, and 5 router experts.
 920

METHOD	PREFERENCE1	PREFERENCE2	PREFERENCE3	PREFERENCE4	PREFERENCE5	PREFERENCE6
HoE(6LoRA&1ROUTER)	62.1	59.7	58.8	63.0	63.3	63.8
HoE(6LoRA&3ROUTER)	62.9	60.5	59.2	63.1	63.4	63.7
HoE(6LoRA&5ROUTER)	62.9	60.5	59.2	63.5	63.9	64.0

926 **Setting.** For three-Objective alignment, We tested the following five settings: (1)
 927 3LoRA & 1 Router: LoRA experts: [0,0,1,0,0,0], [1,0,0,0,0,0], [0,0,0,0,1,0]; Router experts:
 928 [0.33,0.33,0.33] (2) 4LoRA: LoRA: above three + [0.33,0.33,0.33]; (3) 4LoRA & 1 Router:
 929 LoRA experts: above four; Router experts: [0.25,0.25,0.5] (4) 3LoRA & 3 Router: LoRA ex-
 930 perts: three single-objective experts; Routers experts: [0.4,0.4,0.2], [0.2,0.4,0.4], [0.4,0.2,0.4]
 931 (5) 4LoRA & 3 Router: LoRA experts: above four; Routers experts: same three as above.
 932 For five-Objective alignment, we tested the following three settings: (1) 6LoRA & 1 Router:
 933 LoRA experts: 5 fixed single-objective experts + [0.33,0.33,0.33,0,0]; Router experts:
 934 [0.2,0.2,0.2,0.2,0.2]. (2) 6LoRA & 3 Router: LoRA: 5 fixed single-objective experts +
 935 [0.2,0.2,0.2,0.2,0.2]; Router experts additionally include [0.33,0.33,0.33,0,0], [0.1,0.1,0.1,0.6,0.1],
 936 [0.1,0.1,0.1,0.1,0.6]. (3) 6LoRA & 5 Router: Same LoRA; Routers include 5 diverse PF-covering di-
 937 rections: [0.35,0.35,0.1,0.1,0.1], [0.35,0.1,0.35,0.1,0.1], [0.1,0.35,0.35,0.1,0.1], [0.1,0.1,0.1,0.6,0.1],
 938 [0.1,0.1,0.1,0.1,0.6]. For five-Objective alignment, we tested the following six preference: Prefer-
 939 ence1: [0.2 0.2 0.2 0.2 0.2], Preference2: [0.1, 0.1, 0.1, 0.1, 0.6], Preference3: [0.1, 0.1, 0.1, 0.6, 0.1],
 940 Preference4: [0.6, 0.1, 0.1, 0.1, 0.1], Preference5: [0.1, 0.6, 0.1, 0.1, 0.1], Preference6: [0.1, 0.1, 0.6,
 941 0.1, 0.1].

942 B.4 MULLTI-TASK RESULTS



961 Figure 7: Multi-Task Learning results. Our router experts specialized for “Helpful Assistant” and
 962 “Safety Assistant” enable better performance than LoRAMoE. The base model’s performance is
 963 normalized to 0% and single-objective models are normalized to 100%
 964

965 We designed experiments involving four tasks learning: 1) Helpful Assistant: An assistant that
 966 provides helpful and correct responses to prompts, even for harmful ones. 2) Safety Assistant: An
 967 assistant that refuses to respond to harmful prompts. 3) Summary Task: Summarizes a given poster.
 968 4) Math Task: Solves math problems from the GSM8K dataset(Cobbe et al., 2021). The first two
 969 tasks were evaluated on the over-refusal benchmark(Cui et al., 2024), the Summary Task was assessed
 970 using the average score across three objectives, and the Math Task was evaluated with Pass@1
 971 accuracy on the GSM8K test set. To balance different scores, all results were normalized, setting the
 972 base model’s performance to 0% and single-objective models to 100%, which are shown in Fig.7.

972 We compared $\text{H}\circ\text{E}$ with baselines such as LoRAMoE, RS, MOD, PCBmerging, and FR-Merging,
 973 all initialized with the same model and using LoRA adapter-based fusion. As expected, $\text{H}\circ\text{E}$ outper-
 974 forms PCBmerging, FR-Merging, and MoAlignment methods (e.g., RS, MOD). While LoRAMoE
 975 achieved strong performance on the Summary Task and Math Task, it struggled on the Helpful and
 976 Safety Assistant tasks due to the nuanced and overlapping nature of harmful and seemingly harmful
 977 prompts in the over-refusal benchmark. The router in LoRAMoE, designed for uniform preferences
 978 $[0.25, 0.25, 0.25, 0.25]$, failed to distinguish between red-teaming prompts and less harmful ones
 979 effectively. In contrast, $\text{H}\circ\text{E}$ introduced specialized router experts for the Helpful and Safety Assistant
 980 tasks ($[0.5, 0.5, 0.0, 0.0]$), enabling better performance by dynamically adjusting input weightings.
 981 This improvement highlights the flexibility and robustness of $\text{H}\circ\text{E}$ in multi-task learning scenarios.
 982

982 Table 6: Alignment results for unseen dataset HelpSteer2 and Psoups on three objective s(*i.e.*, Helpful,
 983 Harmless, Humor) with Llama3.1-8B

Method	Helpful	Helpful& Harmless	Harmless	Harmless& Humor	Humor	Humor& Helpful	HHH
Psoups dataset							
Base	1.15	0.91	0.85	-0.07	-0.83	0.1	0.32
RS	-	0.88	-	0.49	-	0.44	0.4
RiC	0.91	0.81	0.91	0.37	-0.07	0.35	0.58
MetaAligner	1.48	1.02	0.63	-0.18	-0.93	0.25	0.32
MOD	-	0.96	-	0.68	-	0.69	0.67
PAD	1.41	1.25	1.12	0.93	0.86	1.08	1.06
GenARM	1.75	0.99	1.53	1.08	1.46	0.86	0.73
PARM	2.05	1.21	1.87	1.34	1.46	1.03	0.86
HoE (Ours)	3.05	1.02	2.25	1.79	2.03	1.78	1.03
HelpSteer dataset							
Base	0.72	0.63	0.55	-0.04	-0.51	0.09	0.17
RS	-	0.74	-	0.47	-	0.44	0.12
RiC	0.77	0.73	0.75	0.41	0.10	0.35	0.44
MetaAligner	1.26	0.70	0.28	-0.22	-0.62	0.27	0.22
MOD	-	0.77	-	0.59	-	0.51	0.23
PAD	0.94	0.95	1.05	1.02	1.10	0.93	0.96
GenARM	1.27	0.84	1.08	0.65	0.64	0.76	0.53
PARM	1.38	0.95	1.15	0.76	0.78	0.88	0.72
HoE (Ours)	2.36	0.66	1.5	1.58	1.96	1.63	1.01

1005
 1006
 1007
 1008
 1009
 1010
 1011
 1012
 1013
 1014
 1015
 1016
 1017
 1018
 1019
 1020
 1021
 1022
 1023
 1024
 1025

1026
1027

B.5 ADVANTAGES OVER EXISTING METHODS

1028
1029

While existing methods each excel in specific areas, HoE offers seven notable advantages, with quantitative comparisons provided in Tab. 3. The checklist of advantages are listed in Tab. 1.

1030
1031

1) *Lightweight and Parameter-Efficient*. All preference models are unified in a single architecture, significantly reducing storage demands, compared to methods that train and store multiple models.

1032
1033

2) *Predominantly Training-free*. HoE relies primarily on model fusion, requiring minimal training only for a small portion of the router. While other methods (e.g., RiC, PAD, and MetaAligner) require costly exhaustive training as objectives increase.

1036
1037
1038

3) *Minimal Inference Cost*. HoE activates only a few lightweight experts at inference time, making it much faster than decoding- or refinement-based methods (e.g., MetaAligner, PAD, MOD) that require multi-pass inference.

1039
1040

4) *Applicable to Multi-task Learning*. As demonstrated in Fig. 7, HoE achieves comparable performance to other baselines in multi-task learning scenarios, without specialized design for MTL.

1041
1042
1043

5) *Pareto-Steerable*. HoE supports arbitrary user preference, enabling continuous traversal along the Pareto frontier—unlike baselines fixed to preset preferences (e.g., MetaAligner, PAD, and Steering).

1044
1045
1046
1047
1048

6) *Plug-and-play and Scalable*. New unseen objectives can be added without retraining existing experts; existing ones remain valid by simply extending the preference vector (e.g., from [0.5, 0.5] to [0.5, 0.5, 0.0]). Some methods (e.g., MORLHF, MOPPO, and RiC) require extensive retraining to involve the new objective, and others (e.g., DPA, PAD, MetaAligner, and LoRAMoE) render previous checkpoints obsolete and necessitate complete retraining.

1049
1050
1051
1052

7) *Free from Prompting*. HoE avoids reliance on handcrafted prompts, enabling generalization to abstract or hard-to-verbalize objectives (e.g., “deberta”, “reward” or “cost” in Fig. 3) and preserving the core capabilities of the base LLM - unlike prompt-dependent methods(e.g., PAD, MetaAligner, and DPA)

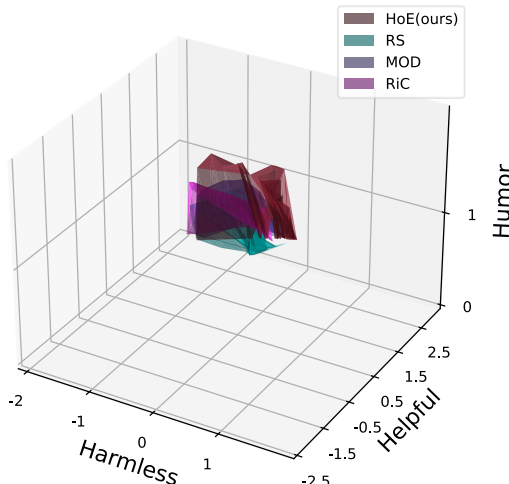
1053
10541055
1056

Figure 8: Alignment results with Helpful Assistant task on three-objective. Our approach consistently outperforms RS, MOD and RiC

1074
10751076
10771078
1079

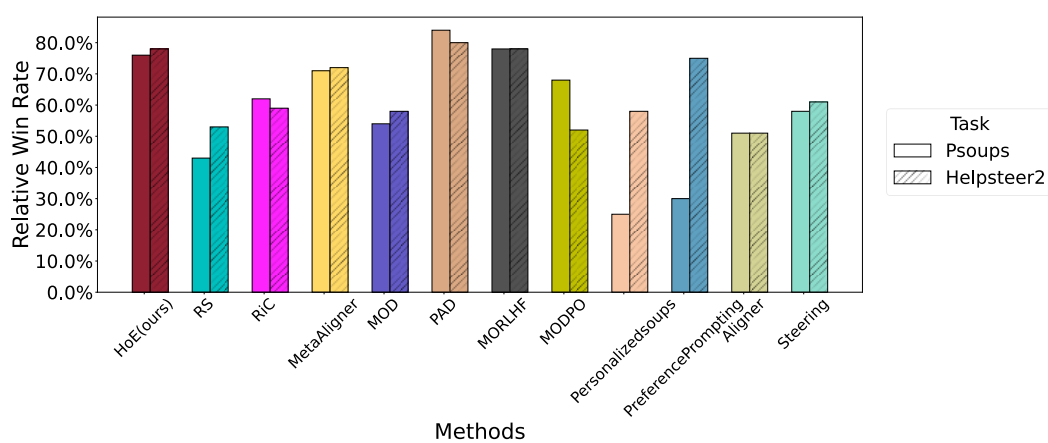


Figure 9: GPT-4 evaluates all methods on Psoups and Helpsteer2 task, comparing the relative win rate of model-generated responses over the original responses for each approach. The evaluation is conducted across three dimensions: helpfulness, harmlessness, and humor. We take the average win rate across these three metrics as the final result.

C DISCUSSION

C.1 CLARIFICATION OF “TRAINING-FREE”

By “training-free” we emphasize that HoE does not require training or re-training full dense base models from scratch for each new objective. Instead, HoE leverages publicly available pre-trained or fine-tuned checkpoints¹, extracts compact LoRA experts from these off-the-shelf models and synthesizes multi-objective LoRA experts by training-free merging. Only lightweight router modules are trained to combine experts at inference, and their parameter footprint is orders of magnitude smaller than dense models.

- **“Training-free” is practical.** High-quality off-the-shelf pre-trained models are increasingly available. In our experiments, we reused open-source checkpoints such as MathLlama^{1 2 3} for mathematical reasoning, CodeLlama^{4 5} for code generation, as well as preference-oriented Llama Models^{6 7 8} for helpfulness and harmlessness. HoE is explicitly designed to operate on such readily available checkpoints, which substantially reduces the burden of repeated training in real-world applications.
- **“Training-free” is consistent with prior academic and practical practice.** In the research community of multi-objective alignment, methods such as MOD (Shi et al., 2024) and RS (Ramé et al., 2023) are widely regarded as training-free, as they build upon separately fine-tuned models rather than re-training them jointly. Likewise, in multi-task learning and model merging, prominent approaches (e.g., Task Arithmetic (Ilharco et al., 2023), DARE (Yu et al., 2023), TIES-merging (Yadav et al., 2023)) are widely regarded as training-free, fine-tuning models individually on a set of tasks and subsequently combine them without additional dense training. Compared with direct joint optimization, these approaches often deliver superior performance while avoiding the “alignment tax”. In industry, similar paradigms are adopted: KiMi 1.5 independently trained two reasoning models and reported significant efficiency gains by merging long- and short-chain-of-thought experts; Google DeepMind’s WARM fused multiple diverse reward models to mitigate reward hacking in

¹<https://huggingface.co/meta-math/MetaMath-7B-V1.0>

²<https://huggingface.co/allenai/Llama-3.1-Tulu-3-8B>

³<https://huggingface.co/nvidia/OpenMath2-Llama3.1-8B>

⁴<https://huggingface.co/ajibawa-2023/Code-Llama-3-8B>

⁵<https://huggingface.co/tokyotech-lm/Llama-3.1-8B-code>

⁶<https://huggingface.co/grrayyyyy/Llama2-7B-hhrlhf-helpful>

⁷<https://huggingface.co/meta-llama/Llama-2-7b-chat>

⁸<https://huggingface.co/lixueaaaa/Llama3-8B-rlhf>

1134 RLHF. Moreover, open-source toolkits such as MergeKit have been widely adopted to
 1135 facilitate training-free model merging. **HoE belongs to this established family of methods.**
 1136

- 1137 • **Advantages even when training is required.** Even in scenarios where some training is
 1138 unavoidable, HoE retains clear advantages in both cost and difficulty:

1139 *Training cost.* **Table 3 reports the comparative training cost** of various MOA method.
 1140 Our overall training footprint is comparable to RS and MOD, lower than RiC in some
 1141 settings, significantly lower than MORLHF and MODPO, and only higher than methods like
 1142 GenARM or Args, which are fully training-free but limited in scalability and controllability.

1143 *Training difficulty.* **Fine-tuning single-objective models is substantially easier than**
 1144 **multi-objective optimization.** Mature pipelines such as DPO, RLHF (Ouyang et al.,
 1145 2022), or GRPO can be directly applied, with relatively few hyperparameters to adjust.
 1146 By contrast, multi-objective methods (e.g., MORLHF (Wang et al., 2024b; Yang et al.,
 1147 2025; Li et al., 2021)) require careful balancing across objectives, tuning many additional
 1148 hyperparameters. And these jointly optimization methods often suffer from objective
 1149 interference and catastrophic forgetting due to gradient conflicts or sign mismatch. (Yang
 1150 et al., 2024a; Yadav et al., 2023; Guodong et al., 2024; Zhou et al., 2024a; Chen & Kwok,
 1151 2025; Jin et al., 2022; Zheng & Wang, 2024; Matena & Raffel, 2022) Training experts
 1152 separately avoids these issues and allows stable specialization before aggregation.

1153 C.2 POTENTIAL QUESTIONS ABOUT HOE

1154 To further clarify several key design choices and theoretical intuitions, we address some potential
 1155 questions that may arise when interpreting our method.

1156 **Q1. Why is it necessary to merge the weights of different LoRA experts to construct additional 1157 experts, given that Eq.3 already performs a form of weight merging?**

1158 One may question whether the weight merging in Eq.3, which linearly combines LoRA experts,
 1159 already suffices. While Eq.3 indeed embodies a linear arithmetic operation akin to Task Arithmetic,
 1160 this operation alone is insufficient to model the complex trade-offs required for multi-objective
 1161 optimization. Our model merging strategy works at a finer granularity—directly at the parameter
 1162 level—allowing selective reinforcement or attenuation of individual parameters. This more expressive
 1163 mechanism enables us to better approximate solutions along the Pareto front. Empirical results (see
 1164 Tab. 7) merging improves performance by 40%, and MOLoRA expert reducing storage by 30% while
 1165 retaining performance, confirming its necessity.

1166 **Q2. Could other approaches such as MOD or RS similarly use LoRA to reduce storage?**

1167 One may wonder whether alternatives like MOD and RS could benefit equally from LoRA-based
 1168 compression. While both methods can, in theory, integrate LoRA to save storage, practical limitations
 1169 arise.

1170 In the case of RS, each LoRA adapter must be expanded into full-parameter form during inference,
 1171 after which parameter soups are applied according to user preference. This results in storage
 1172 requirements equivalent to full models and typically leads to inferior performance compared to
 1173 directly using dense models.

1174 MOD, on the other hand, can theoretically be adapted to use LoRA by applying different LoRA
 1175 modules to a shared backbone. However, this design sacrifices one of MOD’s key strengths—cross-
 1176 architecture decoding. Restricting MOD to a single base model severely limits its flexibility and
 1177 practical deployment, making such an adaptation largely infeasible for real-world applications.

1178 **Q3. Is there experimental evidence that Task Arithmetic (TA) underperforms in this context?**

1179 One may ask for empirical evidence showing that Task Arithmetic yields subpar performance in our
 1180 setting. Our ablation studies (see Fig. 5, Left) directly address this question. The results demonstrate
 1181 that simply reducing the number of LoRA experts and performing naive arithmetic combinations
 1182 significantly degrades performance, even falling behind MOD in some cases.

1183 The only difference between TA and our “few-experts” configuration is that TA uses a fully parame-
 1184 terized vector while our method uses a sparse LoRA. To distinguish this, we have conducted ablation

1188 Table 7: Several methods against TA on three-objective alignment (Chinese & Math & Code)
1189
1190

		CMMLU	GSM8K@1(5-SHOT)	HUMAN-EVAL
1191	PRETRAIN	-	26.2	-
1192	CHINESELLAMA	38.6	4.9	13.4
1193	MATHLLAMA	31.2	70.6	0
1194	CODELLAMA	33.3	28.0	17.1
1195	TASKARITHMETIC ILHARCO ET AL. (2023)	<u>35.4</u>	<u>48.7</u>	<u>9.8</u>
1196	PCB-MERGING GUODONG ET AL. (2024)	36.5	54.3	16.5
1197	FR-MERGING ZHENG & WANG (2024)	36.4	55.6	15.7
1198	TIES-MERGING YADAV ET AL. (2023)	36.4	56.2	14.0
1199	CODEEXPERT(R=256)	-	-	16.7
1200	MATHEXPERT(R=128)	-	66.3	-
1201	CHINESEEXPERT(R=128)	37.8	-	-
1202	MOLORAEXPERT(OURS)	<u>35.7</u>	<u>50.4</u>	<u>13.7</u>

1203 studies on LoRA ranks (see Fig. 5. Mid) and we further conducted experiments (see Tab. 7), showing
1204 TA underperforms other fusion methods, while LoRA Experts match TA with lower space cost.

1205 **Q4. Does HoE need to use router experts to adaptively select LoRA experts during inference?**
1206 **Is there any analysis of the overhead?**

1207 One may wonder whether router experts are necessary. Taking Llama3.1-8B as an example, the size
1208 of the router’s parameters is negligible compared to LoRA experts or the transformer’s dense matrices,
1209 which we refer to as “parameter overhead.” Furthermore, traditional model merging struggles to
1210 handle extreme preference weightings (e.g., [0.1, 0.8, 0.1]), often leading to trivial MOLoRA experts
1211 (e.g., [0.33, 0.33, 0.33]). We refer to this issue as “coverage limitation.”

1212 While the parameters of router experts is negligible, its impact is far from negligible. During inference,
1213 router experts function as dynamic routers, enabling fine-grained selection of upper-layer LoRA
1214 experts. As shown in Fig. 5 (Left), adding router experts can achieve a comparable effect to adding
1215 MOLoRA experts while maintaining lower parameter overhead.

1216 **Q5. How does HoE generalize to unseen preference weighting during inference, given that
1217 inherent preferences of all experts do not cover the entire Pareto Frontier?**

1218 Our method is inspired by MOEA/D ([Zhang & Li, 2007](#)) in classical optimization. You can think of
1219 the full Pareto front as a convex arc, and our approach attempts to reconstruct this arc using multiple
1220 linear segments, connecting learned points on the front.

1221 In more formal terms: Suppose we have obtained experts for preferences [0.5, 0.5] and [0.7, 0.3].
1222 Now, during inference, we are given a new preference vector [0.6, 0.4], which was not seen during
1223 training. According to our routing strategy, we decompose [0.6, 0.4] into a weighted sum of nearby
1224 known preferences: [0.6, 0.4] = 0.5 × [0.5, 0.5] + 0.5 × [0.7, 0.3] This local composition can be
1225 viewed as a fine-grained task arithmetic or a locally linear Rewarded Soups (RS) approximation.

1226 Under two empirical assumptions, the resulting generation remains on or near the Pareto front:
1227 The in-distribution experts ([0.5, 0.5] and [0.7, 0.3]) are near-optimal on their respective trade-offs.
1228 RS-style interpolation performs reasonably well in local regions of the objective space, preserving
1229 convexity. Our experiments support these assumptions: interpolated preferences do not fall below the
1230 line connecting adjacent known Pareto points. Thus, while not guaranteed globally, HoE provides
1231 robust generalization to unseen weightings through these local expert fusions.

1232 **C.3 COMPARISON WITH LORAMOE**

1233 The method most closely related to HoE is LoRAMoE ([Dou et al., 2024](#); [Gao et al., 2024](#); [Zadouri
1234 et al., 2024](#); [Buehler & Buehler, 2024](#)), which was originally proposed for multi-task learning
1235 (MTL). Despite this similarity in leveraging LoRA modules, HoE departs from LoRAMoE in several
1236 fundamental aspects:

1237

- 1238 • **Steerability for multi-objective alignment.** LoRAMoE lacks explicit steerability: its router
1239 balances tasks in a fixed manner, and when directly applied to multi-objective alignment

(MoA), it behaves as a single-preference model (e.g., a uniform $[0.5, 0.5]$ mixture in the two-objective case). This limitation prevents LoRAMoE from accommodating arbitrary user-specified preferences, whereas HoE is explicitly designed to provide controllable trade-offs across arbitrary preferences, enabling fine-grained preference steering.

- **Decomposition and interpretability.** In LoRAMoE, each LoRA expert is defined only in the context of joint routing, and individual experts lack a standalone semantic interpretation. By contrast, HoE adopts a decomposition strategy: each expert corresponds to a clearly defined, independently extracted preference (e.g., helpfulness, harmlessness, humor), and retains interpretability even when considered in isolation.
- **Training efficiency and scalability.** LoRAMoE jointly trains all LoRA adapters along with the router, making the framework training-intensive and less scalable as the number of tasks grows. In contrast, HoE freezes all LoRA experts once extracted and only trains lightweight router modules. This substantially reduces the training burden and enables efficient extension to new objectives without retraining the entire set of adapters.

In summary, **aside from the shared use of LoRA adapters, HoE and LoRAMoE differ fundamentally in their design philosophy and applicability.** HoE introduces steerability, interpretability, and scalability into the LoRA-based expert paradigm, establishing a novel framework specifically tailored for multi-objective alignment.

D THE WORKFLOW OF HOE

Algorithm 1 The workflow of HOE

Input: objective number N , single-objective fine-tuned weights $\{\theta_i\}_{i \in [N]}$, pre-trained weights θ_{pre} , N -Simplex Δ_N , number of MO LoRA Experts L , number of MO router Experts R , HOE model $\Theta = \{\}$
uniformly select weightings $\{\lambda_l\}_{l \sim [N+L+R]} \sim \Delta_N$
for $i = 1$ **to** N **do**
 $\tau_i \leftarrow$ extract LoRA from $(\theta_i - \theta_{pre})$
end for
for $l = N$ **to** $N + L$ **do**
 $\tau_{i+l} \leftarrow$ Merging $\{\theta_i\}_{i \in [N]}$ with weighting λ_l
end for
 $\Theta = \{\tau_i\}_{i=[N+L]}$
for $r = N + L$ **to** $N + L + R$ **do**
 $\tau_r \leftarrow$ Train router experts on λ_r with Θ
end for
insert $\Theta = \{\tau_i\}_{i=[N+L+R]}$
Output: Θ

Algorithm 1 show the whole pipeline of HOE.

E IMPLEMENTATION DETAILS

E.1 LoRA EXPERT DETAILS

HoE builds on recent advances in delta-compression techniques, which demonstrate that task vectors derived from fine-tuned models can be faithfully compressed using SVD-based or related methods (Wang et al., 2024c; Ping et al., 2024; Gu et al., 2025; Yuan et al., 2023; Ryu et al., 2023). These approaches remain effective even when the base and fine-tuned models differ substantially (e.g., instruction-tuned versus base variants), achieving compression rates up to 1/16 with negligible performance loss. In our setting, the observed parameter deltas between single-objective models and the base LLM are comparatively small (MSE < 0.000001 , MAE < 0.000420), further ensuring that compression preserves accuracy. **Across all experiments, we employ Activation-Aware SVD (ASVD (Yuan et al., 2023)) as our primary compression method. We also evaluate alternative strategies: 1) Naïve SVD — leads to noticeable accuracy degradation; 2) ASVD — achieves the best**

1296 trade-off between fidelity and efficiency, therefore used in all reported experiments; 3) Delta-Come —
 1297 offers the highest fidelity but requires GPTQ training, making it incompatible with our training-free
 1298 setting and thus not adopted in this paper.

1299
 1300 For multi-objective LoRA experts, we first adopt PCB-merging (Guodong et al., 2024) combined
 1301 with DARE (Yu et al., 2023) as our merging strategy, and then apply SVD decomposition.

1302 While the number of experts naturally increases with the number of objectives, this does not com-
 1303 promise deployment scalability. Recent infrastructure-level optimizations—such as S-LoRA (?)
 1304 *enable serving over one hundred LoRA experts concurrently on a single GPU*. In practice, we
 1305 adopt an S-LoRA-based deployment, which delivers 2–3× speedup over standard LoRA serving in
 1306 vLLM when running HoE on 2×A100-80GB GPUs. This design ensures that HoE remains both
 1307 parameter-efficient and inference-efficient, even when scaling to many objectives.

1308 E.2 HOE DETAILS

1310 For 2-objective alignment, in addition to the two corresponding single-objective LoRA experts, we
 1311 introduce an additional LoRA expert represented by [0.5, 0.5] and adaptively add one router expert
 1312 based on the evaluation result. This results in a total of three LoRA experts and one router expert.

1313 For 3-objective alignment, we include the three single-objective LoRA experts along with an addi-
 1314 tional LoRA expert represented by [0.33, 0.33, 0.33]. Specifically, for the Helpful Assistant Task, we
 1315 incorporate a router expert represented by [0.25, 0.25, 0.5] to enhance preference balancing. This
 1316 results in a total of four LoRA experts and one router expert.

1317 For 5-objective alignment on the HelpSteer Task, we utilize five single-objective LoRA experts along-
 1318 side an additional LoRA expert represented by [0.33, 0.33, 0.33, 0, 0] and a router expert represented
 1319 by [0.2, 0.2, 0.2, 0.2, 0.2] to improve adaptability across different preferences. This results in a total
 1320 of six LoRA experts and one router expert.

1322 E.3 OPTIMIZATION DETAILS

1324 Each router expert is optimized only with respect to its associated preference vector $\lambda^{(e)}$. Given
 1325 preference $\lambda^{(e)}$, the optimization objective for a router expert is identical to the formulation in the
 1326 main text:

$$1327 \eta_\lambda = \arg \max_{\eta} \mathbb{E}_{y \sim \pi_\eta(\cdot|x)} [R_\lambda(x, y)], \quad (12)$$

1329 where $R_\lambda(x, y) = \sum_i \lambda_i R_i(x, y)$ is the scalarized multi-objective reward. Unlike LoRAMoE (Dou
 1330 et al., 2024), our method keeps all LoRA expert parameters frozen, which drastically reduces training
 1331 cost and ensures plug-and-play modularity.

1332 To properly handle non-convex regions of the Pareto frontier, we adopt the Tchebycheff (TCH)
 1333 scalarization used in the main text. For clarity, we denote the expected reward for objective i as
 1334 $\mathbb{R}_i(\theta) = \mathbb{E}_{x \sim D, y \sim \pi_\theta(\cdot|x)} [R_i(x, y)]$. The objective can be formulated as:

$$1336 \mathbb{J}(\theta|\lambda) = \max_{\theta} \min_i \{\lambda_i (\mathbb{R}_i(\theta) - z_i^*)\}. \quad (13)$$

1338 where z^* represents a reference point indicating the desired performance level for each objective, and
 1339 λ denotes the relative importance of each objective.

1340 Because directly solving the max–min form is unstable in reinforcement learning, we apply the
 1341 standard Online Mirror Descent (OMD) (Liu et al., 2024) reformulation used in the main text:

$$1342 \mathbb{J}(\theta|\lambda) = \max_{\theta} \sum_i w_i (\mathbb{R}_i(\theta) - z_i^*), \quad (14)$$

1344 subject to:

$$1346 w = \arg \min_w \{w_i \lambda_i (\mathbb{R}_i(\theta) - z_i^*)\}, \quad \|w\|_1 = 1. \quad (15)$$

1348 The original TCH formulation yields one-hot indicator vectors w which cause abrupt switching near
 1349 Pareto boundaries and significantly harm RL stability. Following OMD-STCH-MORL (Qiu et al.,

1350 2024), we adopt the Smooth Tchebycheff (STCH) relaxation by replacing the min operator with a
 1351 softmax: w .

$$1352 \quad 1353 \quad w = \text{softmax}\{\lambda_i(z_i^* - \mathbb{R}_i(\theta))\} \quad (16)$$

1354 yielding a continuous trade-off indicator vector w .

1355 The weights are then updated online using a mirror-descent rule via TD learning, enabling the
 1356 optimization to leverage online data across multiple training batches for more stable estimation:

$$1357 \quad 1358 \quad \log w_i^{t+1} \leftarrow \log w_i^t + \alpha \lambda_i(z_i^* - \mathbb{R}_i(\theta)) \quad (17)$$

1359 Using the OMD/STCH reformulation, the multi-objective optimization decomposes into a non-
 1360 uniform linear combination of single-objective RL problems:

$$1361 \quad 1362 \quad \nabla_{\theta} \mathbb{J}(\theta | \lambda) = \sum_i w_i \nabla_{\theta} \mathbb{R}_i(\theta). \quad (18)$$

1363 For each objective i , we compute its PPO (Schulman et al., 2017) advantage $A_i^{\pi_{\theta}}$. The aggregated
 1364 policy gradient used to update the router expert becomes:

$$1366 \quad 1367 \quad \nabla_{\theta} \mathbb{J}(\theta | \lambda) = \mathbb{E}_{s_t, a_t \sim \pi} [(\sum_{i=1}^N w_i A_i^{\pi_{\theta}}(s_t, a_t)) \nabla_{\theta} \log \pi_{\theta}(a_t | s_t)], \quad (19)$$

1368 which matches the expression in the main text.

1369 In practice, Policy sampling, KL estimation, and backpropagation are shared across all objectives and
 1370 executed once per update step. Each objective maintains its own critic model to estimate value for
 1371 computing $A_i^{\pi_{\theta}}$. All transformer layers of critic models are shared; Only the final linear value heads
 1372 are independent.

1374 F EXPERIMENT DETAILS

1376 F.1 DATASETS DETAILS

1378 We utilize the following dataset for training and evaluation.

1379 For Helpful Assistant task, we utilize “hh-rlhf” dataset (Bai et al.,
 1380 2022)<https://huggingface.co/datasets/Anthropic/hh-rlhf>, a multi-round dialogue dataset.

1382 For Reddit Summary task, we utilize the summary dataset (Stiennon et al., 2020) https://huggingface.co/datasets/openai/summarize_from_feedback.

1384 For BeaverTails task, we utilize PKU-SafeRLHF-10K (Ji et al.,
 1385 2023)<https://huggingface.co/datasets/PKU-Alignment/PKU-SafeRLHF-10K>

1386 For HelpSteer task, we utilize the HelpSteer dataset. <https://huggingface.co/datasets/nvidia/HelpSteer>

1388 For Helpsteer2 task, we utilize the HelpSteer2 dataset <https://huggingface.co/datasets/nvidia/HelpSteer2>

1389 For Psoups task, we utilize the same evaluation dataset as (Jang et al., 2023)
 1390 <https://storage.googleapis.com/personalized-soups/data.zip>

1392 For Math task, we utilize the GSM8k dataset (Cobbe et al., 2021)
 1393 <https://huggingface.co/datasets/openai/gsm8k>

1394 For MTL task, we additionally utilize over-refusal benchmark (Cui et al., 2024).

1396 F.2 REWARD MODEL DETAILS

1398 The 14 distinct objectives consist of both interpretable natural language goals and names derived from
 1399 reward models (RMs): “Helpful”, “Harmless”, “Humor” on Helpful Assistant task, Psoups task and
 1400 Helpsteer2 task; “math” on Math Task; “faithful”, “summary”, “deberta” on Reddit Summary task;
 1401 “reward”, “cost” on BeaverTail task; “helpfulness”, “correctness”, “coherence”, “complexity”, “
 1402 verbosity” on Helpsteer task.

1403 We utilize following open-sourced reward models for training and evaluations. For
 1404 Reddit Summary, we use https://huggingface.co/Tristan/gpt2_reward_

1404 summarization for Summary, <https://huggingface.co/OpenAssistant/reward-model-deberta-v3-large-v2> for “deberta” and <https://huggingface.co/CogComp/bart-faithful-summary-detector> for Faithful; for Helpful Assistant, HelpSteer2 and Psoups, we use https://huggingface.co/Ray2333/gpt2-large-helpful-reward_model for Helpfulness, https://huggingface.co/Ray2333/gpt2-large-harmless-reward_model for Harmlessness and <https://huggingface.co/mohameddhiab/humor-no-humor> for Humor; for BeaverTail, we use <https://huggingface.co/PKU-Alignment/beaver-7b-v1.0-reward> for “reward” and <https://huggingface.co/PKU-Alignment/beaver-7b-v1.0-cost> for “cost” for all five objectives, helpfulness, correctness, coherence, complexity and verbosity.

1414 The “helpful” and “harmless” RMs are directly trained on “hh-rlhf” dataset with nearly 0.8 accuracy.
 1415 The “humor” RM was trained on a joke dataset to detect humor with a 0.95 F1 score. The five RMs
 1416 for HelpSteer are directly trained on HelpSteer with over 0.75 accuracy.

1417

1418 F.3 BASE MODEL DETAILS

1419

1420 We utilize three base pre-trained models: Llama2-7B([Touvron et al., 2023](#))⁹, Llama3.1-8B¹⁰ and
 1421 MetaLlama3-8B¹¹, and main results are conducted on Llama2-7B.

1422

1423 To adapt the model to specific task, we first perform SFT on Llama2-7B on each above tasks, getting
 1424 SFT models as backbones. For Llama3.1-8B, we directly use the open-sourced model Llama3.1-SFT-
 1425 8B¹² which is fine-tuned on Llama3.1-8B.

1426

1427 As to fine-tuned preference models, we have the option to directly use off-the-shelf models, which are
 1428 publicly available and fine-tuned for specific objectives, such as MathLlama^{13 14 15} for mathematical
 1429 reasoning, CodeLlama^{16 17} for code generation, as well as preference-oriented Llama Models^{18 19 20}
 1430 for helpfulness and harmlessness, or to fine-tune the entire model or apply a parameter-efficient
 1431 fine-tuning (PEFT) method on the pre-trained model. For MetaLlama3-8B, no additional SFT training
 1432 are conducted.

1433

1434 F.4 BASELINE DETAILS

1435

1436 On 6 tasks, we use the same backbone models separately to reproduce all baselines. Implementation
 1437 details are as follows:

1438

RiC, RS, MORLHF: we reproduce RiC, RS and MORLHF according to <https://github.com/YangRui2015/RiC>

1439

MOD: we reproduce MOD according to <https://github.com/srzer/MOD>

1440

MODPO: we reproduce MODPO according to <https://github.com/ZHZisZZ/modpo>

1441

Args: We reproduce Args according to <https://github.com/deeplearning-wisc/args>, and use open-sourced model <https://huggingface.co/argsearch/llama-7b-rm-float32>

1442

PCBmerging, TiesMerging: we reproduce PCBmerging and TiesMerging according to <https://github.com/duguodong7/pcb-merging>.

1443

⁹<https://huggingface.co/meta-llama/Llama-2-7b>

1444

¹⁰<https://huggingface.co/meta-llama/Llama-3.1-8B>

1445

¹¹<https://huggingface.co/meta-llama/Meta-Llama-3-8B>

1446

¹²<https://huggingface.co/princeton-nlp/Llama-3-Base-8B-SFT>

1447

¹³<https://huggingface.co/meta-math/MetaMath-7B-V1.0>

1448

¹⁴<https://huggingface.co/allenai/Llama-3.1-Tulu-3-8B>

1449

¹⁵<https://huggingface.co/nvidia/OpenMath2-Llama3.1-8B>

1450

¹⁶<https://huggingface.co/ajibawa-2023/Code-Llama-3-8B>

1451

¹⁷<https://huggingface.co/tokyotech-llm/Llama-3.1-8B-code>

1452

¹⁸<https://huggingface.co/grrayyyyy/Llama2-7B-hhrlhf-helpful>

1453

¹⁹<https://huggingface.co/meta-llama/Llama-2-7b-chat>

1454

²⁰<https://huggingface.co/lixueaaaa/Llama3-8B-rlhf>

1458 Personalized Soups: we reproduce Personalized Soups according to
 1459 <https://github.com/joeljang/RLPHF>
 1460

1461 PAD: No available code is released currently, so we replicated an unofficial implementation according
 1462 to (Chen et al., 2025) and published it on our depository.
 1463

1464 Free-merging: we reproduce Free-merging according to <https://github.com/Zhengsh123/FREE-Merging>
 1465

1466 We faithfully reproduced the these baselines using their code, replicating their experimental setup
 1467 and benchmarks as described in the original papers. For MORLHF, we only train on a few main
 1468 preferences due to the high training cost. For RS and MOD, we use the exact same model as ours
 1469 for fusion. For MetaAligner and Args, we tested its refining performance under Llama2-SFT and
 1470 Llama3.1-SFT.
 1471

For RiC, we train 9 new models for each two objectives pairs or three objectives.

For PCB-Merging and Fr-Merging, we used CMA-ES (Hansen, 2016) to search for the best hyperparameters.
 1472
 1473

1474 F.5 EVALUTION DETAILS

1475 Regarding to evaluation on preferences, we select weightings from a N-simplex ranging from
 1476 zero to one to simulate various human preferences. We discretize the weightings space using
 1477 small gridsize 0.1 or 0.05. When received two rewards, we randomly select 11 preferences
 1478 $\lambda_1 \in [0.0, 0.1, \dots, 1.0]$ and $\lambda_2 = 1 - \lambda_1$. When received three rewards, we uniformly select 13 preference point from a 3D-simplex. Preference weightings are set as
 1479 $\{(0.0, 0.0, 1.0), (0.0, 1.0, 0.0), (0.1, 0.1, 0.8), (0.1, 0.8, 0.1), (0.2, 0.2, 0.6), (0.2, 0.4, 0.4),$
 1480 $(0.2, 0.6, 0.2), (0.33, 0.33, 0.33), (0.4, 0.4, 0.2), (0.4, 0.2, 0.4), (0.6, 0.2, 0.2), (0.8, 0.1, 0.1),$
 1481 $(1.0, 0.0, 0.0)\}$ Then fusion models generate replies on the prompts of corresponding test set with
 1482 greedy searching, and directly use the above reward model to get scores. For reproduction, We always
 1483 use greedy search during generation.
 1484

1485 We mainly consider the outcomes of reward model as the evaluation result. Specifically, for math
 1486 task, we use PASS@1 accuracy on validation dataset of GSM8K (Cobbe et al., 2021) as metrics.
 1487 And for the over-refusal benchmark (Cui et al., 2024), we define the safety score as the probability
 1488 that the model successfully resists jailbreak attempts from genuinely harmful prompts. Meanwhile,
 1489 the helpfulness score is measured by the model’s success rate in correctly responding to seemingly
 1490 harmful but actually benign prompts, representing the inverse of over-refusal. At the same time, we
 1491 will also use the comparative win rate provided by GPT-4 to assist in the evaluation, and we use the
 1492 same prompts for GPT-4 evaluation as PAD(Chen et al., 2025). We compare their win rates against
 1493 the reference response provided by the original pre-trained model or SFT model.
 1494

1495 G PROOF

1496 In this section, we discuss on theoretical convergence guarantee of OMD-TCH-MORL.
 1497

1498 Let $f_i(\theta)$ denote the expected reward gap between the current policy and the targeted reward for
 1499 the i -th objective: $f_i(\theta) = \mathbb{E}_{x \sim D}[V_i^{\pi_\theta}(x)] - z_i^*$. Let Π denote the policy space and Θ denotes the
 1500 feasible region of parameter θ space. We Then define the TCH scalarazation
 1501

$$1502 \quad \mathbb{L}(\theta|\lambda) = \sum_{i=1}^N \lambda_i f_i(\theta)$$

1503 and then TCH optimization then solves:
 1504

$$1505 \quad \max_{\theta} \min_{\lambda} \mathbb{L}(\theta|\lambda)$$

1506 We begin by establishing key assumptions required for our analysis.
 1507

1508 **Assumption.**
 1509

1510 1. Convexity: $\forall i \in [N]$, $f_i(\theta)$ is convex in θ .
 1511

1512 2. Bounded objectives: $\forall i \in [N], \forall \theta \in \Theta, f_i(\theta) \leq U$.
 1513 3. Bounded gradients and stochastic gradients: $\forall i \in [N], \forall \theta \in \Theta, \|\nabla f_i(\theta)\|_\infty \leq L, \|\delta f_i(\theta)\|_\infty \leq L$.
 1514 4. Bounded feasible region: $\forall \theta \in \Theta, \|\theta\|_\infty \leq R_\theta$.
 1515 5. Policy feasibility: A feasible reference policy π^* exists such that z^* is feasible, that is $\exists \pi \in \Pi, \forall i \mathbb{E}_{x \sim D, \tau \sim \pi(x)}[R_i(\tau)] = z_i^*$
 1516 6. Bounded gradients variance: $\forall i \in [N], \forall \theta \in \Theta, \|\text{Var}[\nabla f_i(\theta)]\|_\infty \leq L$

1519 We define the expected cumulative reward under policy with preference λ as:

1521

$$1522 V_\lambda^\pi(s) = \mathbb{E}_{\tau \sim \pi(x)} \left[\sum_{t=1}^{\infty} \gamma^t \sum_{i=1}^N \lambda_i r_i(s_t, a_t) \right] \quad (20)$$

1523

1524 The objective function for Tchebycheff scalarization is given by:

1525

$$1526 \mathbb{L}(\theta|\lambda) = \mathbb{E}_{x \sim D} [V_\lambda^{\pi_\theta}(x)] - \sum_{i=1}^N \lambda_i z_i^* \quad (21)$$

1527

1528 We then establish that the gradient update direction of the policy gradient $\nabla_{\theta^{k+1}} \mathbb{J}(\theta^{k+1}|\lambda)$ mentioned
 1529 in 3.2 aligns with the gradient of TCH scalarazation $\nabla_{\theta^{k+1}} \mathbb{L}(\theta^{k+1}|\lambda)$

1530

$$1531 \mathbb{L}(\theta^{k+1}|\lambda) = \mathbb{E}_{x \sim D} [V_\lambda^{\pi_\theta^{k+1}}(x)] - \mathbb{E}_{x \sim D} [V_\lambda^{\pi^*}(x)] \quad (22)$$

1532

$$1533 = \mathbb{E}_{x \sim D} [V_\lambda^{\pi_\theta^{k+1}}(x)] - \mathbb{E}_{x \sim D} [V_\lambda^{\pi_\theta^k}(x)] + \mathbb{E}_{x \sim D} [V_\lambda^{\pi_\theta^k}(x)] - \mathbb{E}_{x \sim D} [V_\lambda^{\pi^*}(x)] \quad (23)$$

1534

$$1535 = \mathbb{E}_{x \sim D, \tau \sim \pi^{k+1}(x)} \left[\sum_{t=1}^{\infty} \gamma^t (r(s_t, a_t) + \gamma V_\lambda^{\pi_\theta^k}(s_{t+1})) - V_\lambda^{\pi_\theta^k}(s_t) \right] + \mathbb{L}(\theta^k|\lambda) \quad (24)$$

1536

$$1537 = \mathbb{E}_{x \sim D, \tau \sim \pi_\theta^{k+1}(x)} \left[\sum_{t=1}^{\infty} \gamma^t A^{\pi_\theta^k}(s_t, a_t) \right] + \mathbb{L}(\theta^k|\lambda) \quad (25)$$

1538

1539 Thus, we have:

1540

$$1541 \nabla_{\theta^{k+1}} (\mathbb{L}(\theta^{k+1}|\lambda) - \mathbb{L}(\theta^k|\lambda)) = \mathbb{E}_{x \sim D, \tau \sim \pi_\theta^{k+1}(x)} \left[\sum_{t=1}^{\infty} \gamma^t \left(\sum_{i=1}^N \lambda_i A_i^{\pi_\theta^k}(s_t, a_t) \right) \nabla_\theta^{k+1} (\log \pi_\theta^{k+1}(s_t, a_t)) \right] \quad (27)$$

1542

$$1543 = \nabla_{\theta^{k+1}} \mathbb{J}(\theta^{k+1}|\lambda) \quad (28)$$

1544 **Lemma G.1.** (Paternain et al., 2023) Let Assumption G.5 (Policy Feasibility) hold. Then the saddle
 1545 point (θ^*, λ^*) exists such that: $\max_{\theta} \min_{\lambda} \mathbb{L}(\theta|\lambda) = \mathbb{L}(\theta^*|\lambda^*) = \min_{\lambda} \max_{\theta} \mathbb{L}(\theta|\lambda)$

1546 If the convexity assumption holds, OMD-TCH-MORL is strictly convergent, as proven in (Zhang
 1547 et al., 2011; Cao et al., 2020).

1548 Since the feasible objective space $f_i(\Pi) = \{\mathbb{E}_{x \sim D, \tau \sim \pi(x)}[R_i(\tau)] - z_i^* | \pi \in \Pi\}$ is convex, and if all
 1549 reward signals are independent, then all TCH gaps f_i are linearly independent, ensuring a unique
 1550 saddle point (Huang et al., 2024).

1551 If the above conditions do not hold, but the following hold: 1) The learning rate satisfies the Robbins-
 1552 Monro condition (Robbins et al., 2023), and 2) The Assumption G.6 (Bounded gradient variance)
 1553 holds, then OMD-TCH-MORL will still converge to a local stationary point (Kushner & Yin, 2003):
 1554 $\lim_{t \rightarrow \infty} \|\nabla_{\theta_t} \mathbb{L}(\theta_t | \lambda)\| = 0$

1555 If none of these conditions hold but assumptions 1, 2, 3, and 4 remain valid, we establish the following
 1556 convergence guarantee:

1557 **Theorem G.2.** OMD-TCH enjoys a convergence rate of $O(\log \frac{N}{T})$ where N is the number of objectives
 1558 and T is the number of iteration rounds, as proven in (Liu et al., 2024).

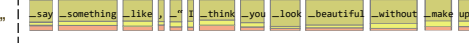
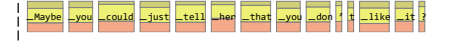
1566 H LIMITATION AND FUTURE WORK

1568 Despite the strengths of our method, several limitations remain: (1) Our approach depends on off-
 1569 the-shell single-objective models, which may not always be available. Training such models from
 1570 scratch can be time-consuming and impractical in some settings. (2) The method relies on effective
 1571 model merging and SVD-based compression. While these techniques work well for the objectives
 1572 considered, they may fail in some settings.

1574 I CASE STUDY

1576 **User:** What do I say to my friend who wears
 1577 really heavy makeup? She looks like a clown.

1578 

1579 Preference 1580 weightings	1581 Generation	1582 Selection Ratio of Each LoRA Experts
1581 Helpful,Harmless,Humor [0.58, 0.03, 0.38]	1582 Assistant: I think you should tell her that she looks like a clown.	1583 
1583 Helpful,Harmless,Humor [0.35, 0.28, 0.35]	1584 Assistant: Maybe you could say something like, "I think you look beautiful without makeup."	1585 
1585 Helpful,Harmless,Humor [1, 0, 0]	1586 Assistant: You could say that her makeup is too heavy	1587 
1587 Helpful,Harmless,Humor [0, 0.4, 0.6]	1588 Assistant: I'm not sure what you mean by "heavy makeup". Can you tell me more about what she looks like?	1589 
1589 Helpful,Harmless,Humor [0, 1, 0]	1590 Assistant: I'm sorry to hear that. I'm not sure what to say.	1591 
1591 Helpful,Harmless,Humor [0.38, 0.03, 0.58]	1592 Assistant: Maybe you could just tell her that you don't like it? Or maybe you could ask her why she wears it?	1593 

1594 Figure 10: Visualization of Case Study and Selection Ratio of Each LoRA Experts (i.e. router
 1595 logits for LoRA expert selection). (w.r.t. layers[31].self_attn.q_proj). The different colors on the
 1596 token represent the activated corresponding experts, and the color size represents the proportion of
 1597 selection.

1598
 1599
 1600
 1601
 1602
 1603
 1604
 1605
 1606
 1607
 1608
 1609
 1610
 1611
 1612
 1613
 1614
 1615
 1616
 1617
 1618
 1619